PHYSICAL REVIEW D VOLUME 23, NUMBER 1 1 JANUARY 1981

Chromodynamic corrections to neutrino production of heavy quarks

Thomas Gottschalk
High Energy Physics Division, Argonne National Laboratory, Argonne, Illinois 60439
(Received 9 June 1980; revised manuscript received 21 July 1980)

The $O(\alpha_s)$ perturbative quantum-chromodynamic corrections to weak, charged-current production of heavy quarks are evaluated. For perturbative subtractions and parton densities defined via the electroproduction structure function $F_2^{\gamma *}$, the residual corrections to νN flavor-production structure functions are shown to be modest except for $x' \to 1$ or $Q^2 \ll M^2$. We investigate sensitivity of the results to different perturbative subtraction prescriptions. Specializing to charm production, we further find that, for $E_\nu > 30$ GeV, color-radiative corrections modify estimated production cross sections by no more than 10%. The results for charm are shown to be generally insensitive to factorization of $G \to c\bar{c}$ splitting "singularities" into evolution of an intrinsic charm-sea component of the nucleon. The longitudinal structure function due to charm production is computed and found to be substantial.

I. INTRODUCTION

Initial optimism that factorized, leading-logarithm perturbative quantum chromodynamics[1] (QCD) might provide a quantitative description of hard-scattering hadronic processes has been tempered somewhat by recent calculations of sizeable nonleading corrections for several processes.[2-6] It is now known that these "large corrections" are very much prescription dependent, and can often be reduced by judicious choices for perturbative subtraction schemes.[7-9] Nonetheless, these results do demonstrate the need for evaluating nonleading color-radiative corrections for as many processes as possible in order to understand the behavior of QCD perturbative expansions and the validity of lowest-order approximations used in hard-scattering phenomenology. In this work we continue such a program by evaluating the chromodynamic corrections to heavy-flavor production by neutrinos.

Beyond simply extending the class of "radiatively corrected" processes, we wish to emphasize the value of neutrino charm production as an accessible laboratory for experimental studies of perturbative QCD. Opposite-sign dileptons provide a clean signal for charm at a substantial fraction of the total neutrino cross section. The observed suppression of same-sign dileptons[10] supports the expectation that soft $c\bar{c}$-hadronization is suppressed. The lepton from charm decay thus provides a clean probe of gluon-bremsstrahlung effects on the production and fragmentation of a *specific, identified* quark. Sufficient data now exist[11] to make quantitative study of such effects a useful complement to jet analyses in e^+e^- annihilation. The $O(\alpha_s)$-corrected structure functions and cross sections presented here constitute first steps in obtaining a normalized, "standard model" for phenomenological comparisons.

The organization of the rest of this work is as follows.

In Sec. II we evaluate the perturbative structure functions for heavy-quark production, using dimensional regularization for infrared and ultraviolet divergences. The perturbative results are presented in the form required for subsequent factorization of initial-state singularities: a known splitting-function coefficient times a simple pole plus a finite residual. Attainment of this form is found to require a slow-rescaling parton-model formalism.

Absorption of the splitting singularities is done in Sec. III. We define the perturbative subtraction scheme using the electroproduction structure function F_2. Perturbative structure functions needed for these subtractions are presented, with particular attention given to the heavy-quark pair-production process, $\gamma^* G \to Q\bar{Q}$. Our final results for the corrected flavor-production structure functions are presented in Sec. III C. We also discuss sensitivity of these results to changes in the perturbative subtraction scale and to treatment of the heavy-quark sea.

In Sec. IV we investigate the radiative corrections for charm production. The fractional changes in the structure functions $F_j(x')$ are small except at very large x'. The estimated changes in the charm-production cross section are also quite small—of order 5% over the energy range relevant for current experiments. These results are shown to be largely insensitive to different treatments of the charm sea. The longitudinal structure function due to charm production is also examined.

Section V summarizes our principal conclusions.

II. PERTURBATIVE CROSS SECTIONS

In this section we compute the elementary cross sections for heavy-flavor production in neutrino-quark and neutrino-gluon scattering to $O(\alpha_s)$.

Since the initial states involve colored quanta, these cross sections contain canonical collinear singularities. The absorption of these singularities into measurable quark and gluon distributions and subsequent calculations of physical cross sections are discussed in Sec. III.

In principle, evaluation of the perturbative cross sections is straightforward. In practice, the nonzero heavy-quark mass results in complications. In particular, care must be taken so that the final expressions agree with known results in the limit $M \to 0$. In Secs. II A and II B we present the perturbative calculations in sufficient detail for our results to be reproduced or generalized without undo effort.

Those readers interested only in the results of the perturbative calculation can skim Secs. II A and B without loss of content.

Hidden in the considerable algebra of Secs. II A and B we do find a few points worthy of separate comment. These are mentioned in Sec. II C.

A. Neutrino-quark scattering

To $O(\alpha_s)$, the contributing processes are

$$\nu(k_1)+q(p_1)\to\mu(k_2)+Q(p_2) \tag{1}$$

and

$$\nu(k_1)+q(p_1)\to\mu(k_2)+Q(p_2)+G(p_3) \tag{2}$$

corresponding to the graphs shown in Fig. 1. Throughout, we use Q (q) to denote a massive (massless) quark, with $p_2^{\,2}\equiv M^2$.

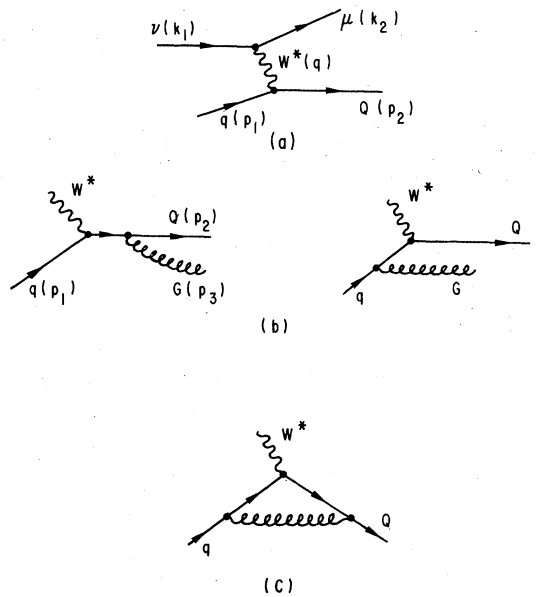

FIG. 1. Graphs contributing to $W^*q\to QX$ through $O(\alpha_s)$.

The amplitude for the Born term, Fig. 1(a), is written as

$$\mathfrak{M}_0=\frac{\kappa G_F}{\sqrt{2}}\,l^\alpha h^\alpha, \tag{3}$$

where, as usual

$$l^\alpha=\bar u(k_2)\gamma^\alpha(1-\gamma_5)u(k_1), \tag{4}$$

$$h^\alpha=\bar u(p_2)\gamma^\alpha(1-\gamma_5)u(p_1), \tag{5}$$

and κ is the $q\to Q$ weak coupling relative to $(G_F/\sqrt{2})^{1/2}$. The cross section is then

$$\frac{d\sigma}{dQ^2}=\frac{\kappa^2 G_F^{\,2}}{64\pi\hat s^2}L^{\alpha\beta}H^{\alpha\beta}, \tag{6}$$

with

$$\hat s\equiv(p_1+k_1)^2, \tag{7}$$

$$Q^2\equiv -q^2=-(k_1-k_2)^2, \tag{8}$$

and

$$L^{\alpha\beta}\equiv\sum_{\text{spins}} l^{\alpha\dagger}l^\beta$$
$$=8(k_1^\alpha k_2^\beta+k_2^\alpha k_1^\beta-k_1\cdot k_2\,g^{\alpha\beta}+i\epsilon_{\alpha\beta\mu\nu}k_1^\mu k_2^\nu). \tag{9}$$

The hadronic tensor $H^{\alpha\beta}$ is similar to Eq. (9). However, to establish connections with higher-order terms, we write this as

$$H^{\alpha\beta}=-4(Q^2+s)H_1 g^{\alpha\beta}+16H_2 p_1^\alpha p_1^\beta+8iH_3\epsilon_{\alpha\beta\mu\nu}p_1^\mu q^\nu$$
$$+8H_4 q^\alpha q^\beta+8H_5(q^\alpha p_1^\beta+p_1^\alpha q^\beta), \tag{10}$$

where $s=(k_1+p_1-k_2)^2$ is the squared mass of the recoil system. The functions H_j are related to conventional deep-inelastic structure functions by coupling strengths and a convolution with nonperturbative parton densities, as discussed in Sec. III. For the Born term, Eq. (1),

$$H_1=H_2=H_3=H_5=1,\qquad H_4=0. \tag{11}$$

This specifies our normalization.

For the real-gluon emission process, Eq. (2), we write

$$\mathfrak{M}=\left(\frac{\kappa G_F}{\sqrt{2}}\right)gT^a l^\alpha H^\alpha, \tag{12}$$

where g is the QCD coupling, T^a is a color matrix, and

$$H^\alpha=(h_1^{\alpha\mu}+h_2^{\alpha\mu})\epsilon^{\mu *}, \tag{13}$$

with

$$(2p_2\cdot p_3)h_1^{\alpha\mu}=\bar u(p_2)\gamma^\mu(\not p_2+\not p_3+M)\gamma^\alpha(1-\gamma_5)u(p_1),$$
$$(-2p_1\cdot p_3)h_2^{\alpha\mu}=\bar u(p_2)\gamma^\alpha(1-\gamma_5)(\not p_1-\not p_3)\gamma^\mu u(p_1) \tag{14}$$

corresponding to the graphs in Fig. 1(b). Main-

taining the normalization of Eq. (6), we obtain

$$H^{\alpha\beta} = \langle \tfrac{4}{3} \rangle \frac{g^2}{2\pi} \int ds\, d_2 P(p_1 + q \to p_2 + p_3) \times \sum_{\text{spin}} H^{\alpha\dagger} H^{\beta}, \tag{15}$$

where

$$s \equiv (p_1 + q)^2 \tag{16}$$

and $d_2 P$ is the usual $2 \to 2$ phase-space factor. The factor $\langle \frac{4}{3} \rangle$ in Eq. (15) arises from color averaging.

To control the infrared divergences contained in Eq. (15), we use the techniques of dimensional regularization.[12] That is, we evaluate Eq. (15) in space-time dimension

$$D \equiv 4 + 2\epsilon . \tag{17}$$

The infrared singularities in $H^{\alpha\beta}$ then appear as $1/\epsilon$ poles. Using this method, we can consistently calculate with *on-shell* external particles [as is implicit in Eq. (14)]. This both simplifies phase-space integrations and maintains gauge invariance at all intermediate stages of the calculation.[13]

We compute $H^{\alpha\beta}$ by projecting out the individual structure functions H_j:

$$H_j = P_j^{\alpha\beta} H^{\alpha\beta} = \frac{2g^2}{3\pi} (\mu^{-2\epsilon}) ds\, d_2 P P_j^{\alpha\beta} \left(\sum_{\text{spin}} H^{\alpha\dagger} H^{\beta} \right). \tag{18}$$

The mass parameter μ keeps the coupling g dimensionless in D dimensions, $g \to g\mu^{-\epsilon}$. The projection operators are given in Appendix B. We will evaluate H_1 in some detail, and simply quote results for the other H_j. The integrand in Eq. (18) for H_1 is

$$P_1^{\alpha\beta} \left(\sum_{\text{spins}} H^{\alpha\dagger} H^{\beta} \right) \equiv \left(\frac{1}{s - M^2} \right) H_1', \tag{19}$$

with

$$H_1' = -4 \left[\frac{s(Q^2 + M^2)}{(s - M^2)(Q^2 + s)} - \frac{(1 - \epsilon)(s - M^2)}{Q^2 + s} + \left(\frac{s - M^2}{Q^2 + s} \right)^2 + \frac{(1 + \epsilon)t}{2(s + Q^2)} - \frac{st(Q^2 + M^2)}{(s + Q^2)^3} + \frac{Q^2 + M^2}{t} + \frac{(1 + \epsilon)(s - M^2)^2}{2t(s + Q^2)} \right], \tag{20}$$

where $t \equiv (p_1 - p_3)^2$, and we have discarded $O(\epsilon^2)$ terms in H_1' which do not contribute to the final result for H_1.

In $D = 4 + 2\epsilon$ dimensions, the two-body phase space factor is

$$d_2 P = \frac{1}{8\pi} \frac{s - M^2}{s} \frac{1}{\Gamma(1 + \epsilon)} \left[\frac{(s - M^2)^2}{4\pi s} \right]^{\epsilon} dy [y(1 - y)]^{\epsilon}, \tag{21}$$

where

$$y \equiv \tfrac{1}{2}(1 + \cos\theta_{13}^{*}) \tag{22}$$

so that

$$t = -\left(\frac{1}{s} \right) (s + Q^2)(s - M^2)(1 - y) . \tag{23}$$

The y integrations are easily performed, giving β functions. Before giving results, it is convenient to introduce notation:

$$z \equiv \frac{Q^2 + M^2}{Q^2 + s} , \tag{24}$$

$$\lambda \equiv \frac{Q^2}{Q^2 + M^2} , \tag{25}$$

$$\xi \equiv \frac{s - M^2}{s} = \frac{1 - z}{1 - \lambda z} . \tag{26}$$

We then have

$$\int_0^1 dy [y(1 - y)]^{\epsilon} H_1' \equiv 2 \frac{\Gamma^2(1 + \epsilon)}{\Gamma(1 + 2\epsilon)} \left(\frac{s}{s - M^2} \right) H_1'' , \tag{27}$$

with

$$H_1'' = \frac{1 + z^2}{\epsilon} + 1 - 4z + z^2 + 4\epsilon z + \xi z(1 - z) - 2\xi\epsilon(1 - z^2) + \tfrac{1}{2}\xi^2(1 - \epsilon) , \tag{28}$$

where we have dropped terms $O(\epsilon^2)$. Collecting terms gives

$$H_1 = \left\langle \frac{4}{3} \right\rangle \frac{\alpha_s}{2\pi} \left(\frac{Q^2 + M^2}{4\pi\mu^2} \right)^{\epsilon} \frac{\Gamma(1 + \epsilon)}{\Gamma(1 + 2\epsilon)} \times \frac{dz}{z} (1 - z)^{2\epsilon - 1} (1 - \lambda z)^{-\epsilon} z^{-\epsilon} H_1''(z, \xi, \epsilon) . \tag{29}$$

Next it is convenient to rewrite the $(1 - z)^{2\epsilon - 1}$ singularity using the identities

$$(1 - z)^{2\epsilon - 1} z^{-\epsilon} (1 - \lambda z)^{-\epsilon} = \delta(1 - z) \left[\frac{1}{\epsilon} - \frac{(1 - \lambda)^{\epsilon}}{2\epsilon} - \epsilon \operatorname{Li}_2(\lambda) \right] + \left[\frac{1}{1 - z} \right]_+ - \frac{\epsilon \ln z}{1 - z} + \epsilon \left[\frac{2\ln(1 - z) - \ln(1 - \lambda z)}{1 - z} \right]_+ + O(\epsilon^2) , \tag{30}$$

$$(1 - z)^{2\epsilon - 1} (1 - \lambda z)^{-\epsilon} \xi = \delta(1 - z) \left[\frac{1}{\epsilon} - \frac{(1 - \lambda)^{\epsilon}}{\epsilon} - K_A \right] + \left[\frac{1}{1 - \lambda z} \right]_+ + O(\epsilon) , \tag{31}$$

$$(1 - z)^{2\epsilon - 1} (1 - \lambda z)^{-\epsilon} \xi^2 = \delta(1 - z) \left[\frac{1}{\epsilon} - \frac{(1 - \lambda)^{\epsilon}}{\epsilon} - \frac{1 + \lambda}{\lambda} K_A - \frac{1}{\lambda} \right] + \left[\frac{1 - z}{(1 - \lambda z)^2} \right]_+ + O(\epsilon) , \tag{32}$$

where

$$K_A \equiv \frac{1}{\lambda}(1-\lambda)\ln(1-\lambda)\,, \tag{33}$$

Li_2 is the usual dilogarithm,

$$\mathrm{Li}_2(x) \equiv -\int_0^1 \frac{dy}{y}\ln(1-xy)\,, \tag{34}$$

and, for arbitrary $h(z)$, the corresponding distribution $[h(z)]_+$ is defined by its integrals:

$$\int_0^1 dz\, f(z)[h(z)]_+ \equiv \int_0^1 dz[f(z)-f(1)]h(z)\,. \tag{35}$$

Note that, for $\epsilon \to 0$, the left-hand side of Eq. (31) is simply $(1-\lambda z)^{-1}$ and appears to require no regularization. However, replacing Eqs. (31) and (32) by their $\epsilon = 0$ values results in a final expression for H_1 which does not have a well defined massless limit. [For example, Eq. (40) acquires an uncanceled $\delta(1-z)\delta(1-\lambda)$ piece.] The expansions in Eqs. (31) and (32) are necessary if Eq. (40) is to agree with the known massless result for $\lambda \to 1$.

Using Eqs. (30)–(32) in Eq. (29), we obtain

$$H_1^R = \langle \tfrac{4}{3} \rangle \frac{\alpha_s}{2\pi}\left(\frac{Q^2+M^2}{4\pi\mu^2}\right)^{\epsilon} \frac{\Gamma(1+\epsilon)}{\Gamma(1+2\epsilon)} \frac{dz}{z}\left\{\delta(1-z)\left[\left(\frac{-1}{\epsilon^2}+\frac{1}{2\epsilon}-\frac{3}{2}\right)(1-\lambda)^{\epsilon}+\frac{2}{\epsilon^2}-\frac{3}{2\epsilon}+\frac{7}{2}-\frac{1}{2\lambda}-2\,\mathrm{Li}_2(\lambda)-\left(\frac{1+\lambda}{2\lambda}\right)K_A\right]\right.$$
$$+\frac{1}{\epsilon}\,\frac{1+z^2}{(1-z)_+}-\frac{(1+z^2)\ln z}{1-z}+(1+z^2)\left[\frac{2\ln(1-z)-\ln(1-\lambda z)}{1-z}\right]_+$$
$$\left.+(1-4z+z^2)\left[\frac{1}{1-z}\right]_+ + z(1-z)\left[\frac{1}{1-\lambda z}\right]_+ + \frac{1}{2}\left[\frac{1-z}{(1-\lambda z)^2}\right]_+ + O(\epsilon)\right\}. \tag{36}$$

To obtain the complete $O(\alpha_s)$ correction to H_1, we must add the contributions H_1^V from the virtual graphs in Fig. 1(c). These virtual terms are calculated in Appendix A, with the result

$$H_1^V = \left\langle \frac{4}{3} \right\rangle \frac{\alpha_s}{2\pi}\left(\frac{Q^2+M^2}{4\pi\mu^2}\right)^{\epsilon} \frac{\Gamma(1+\epsilon)}{\Gamma(1+2\epsilon)}\,\delta(1-z)\left[\left(\frac{1}{\epsilon^2}-\frac{1}{2\epsilon}+2\right)(1-\lambda)^{\epsilon}-\frac{2}{\epsilon^2}+\frac{3}{\epsilon}-8-K_A+2\,\mathrm{Li}_2(\lambda)-\frac{\pi^2}{3}\right]. \tag{37}$$

Combining terms and adding the $\delta(1-z)$ contribution from the Born term, Eq. (11), we obtain

$$H_1 = \frac{dz}{z}\left[\delta(1-z)+\frac{1}{\epsilon}\left(\frac{Q^2+M^2}{4\pi\mu^2}\right)^{\epsilon}\frac{\Gamma(1+\epsilon)}{\Gamma(1+2\epsilon)}\,\frac{\alpha_s}{2\pi}\,P_{q/q}(z)+\frac{\alpha_s}{2\pi}\,h_{1,q}+O(\epsilon)\right], \tag{38}$$

where[14]

$$P_{q/q}(z) = \left\langle \frac{4}{3} \right\rangle\left[\frac{3}{2}\,\delta(1-z)+\frac{1+z^2}{(1-z)_+}\right] \tag{39}$$

is the usual quark-in-a-quark splitting function, and the residual term $h_{1,q}$ is

$$h_{1,q} = \left\langle \frac{4}{3} \right\rangle\left\{-\delta(1-z)\left(4+\frac{1}{2\lambda}+\frac{\pi^2}{3}+\frac{1+3\lambda}{2\lambda}K_A\right)-\frac{(1+z^2)\ln z}{1-z}+(1+z^2)\left[\frac{2\ln(1-z)-\ln(1-\lambda z)}{1-z}\right]_+\right.$$
$$\left.+(1-4z+z^2)\left[\frac{1}{1-z}\right]_+ + z(1-z)\left[\frac{1}{1-\lambda z}\right]_+ + \frac{1}{2}\left[\frac{1-z}{(1-\lambda z)^2}\right]_+\right\}. \tag{40}$$

To quote results for all structure functions, we first define

$$\mathcal{P}_q(z) \equiv \delta(1-z)+\frac{1}{\epsilon}\left(\frac{Q^2+M^2}{4\pi\mu^2}\right)^{\epsilon}\frac{\Gamma(1+\epsilon)}{\Gamma(1+2\epsilon)}\,\frac{\alpha_s}{2\pi}P_{q/q}(z)\,. \tag{41}$$

Then

$$H_1^q(z) = \frac{dz}{z}\left[\mathcal{P}_q(z)+\frac{\alpha_s}{2\pi}\,h_{1,q}(z,\lambda)\right],$$
$$H_2^q(z)/z = \frac{dz}{z}\left[\mathcal{P}_q(z)+\frac{\alpha_s}{2\pi}h_{2,q}(z,\lambda)\right],$$
$$H_3^q(z) = \frac{dz}{z}\left[\mathcal{P}_q(z)+\frac{\alpha_s}{2\pi}h_{3,q}(z,\lambda)\right], \tag{42}$$
$$H_4^q(z) = \frac{dz}{z}\left[\frac{\alpha_s}{2\pi}h_{4,q}(z,\lambda)\right],$$
$$H_5^q(z) = \frac{dz}{z}\left[\mathcal{P}_q(z)+\frac{\alpha_s}{2\pi}h_{5,q}(z,\lambda)\right],$$

where the superscript q designates quark-current scattering. Note that H_4^q has no initial-state singularities. We expand the residuals $h_{j,q}$ as

$$h_{j,q} = \langle \tfrac{4}{3} \rangle\left\{h_q + A_j\delta(1-z)\right.$$
$$+B_1^j\left[\frac{1}{1-z}\right]_+ + B_2^j\left[\frac{1}{1-\lambda z}\right]_+$$
$$\left.+B_3^j\left[\frac{1-z}{(1-\lambda z)^2}\right]_+\right\}, \tag{43}$$

with

$$h_q = -\left(4+\frac{1}{2\lambda}+\frac{\pi^2}{3}+\frac{1+3\lambda}{2\lambda}K_A\right)\delta(1-z)-\frac{(1+z^2)\ln z}{1-z}$$
$$+(1+z^2)\left[\frac{2\ln(1-z)-\ln(1-\lambda z)}{1-z}\right]_+, \tag{44}$$

with K_A as defined in Eq. (33). Coefficients for $j = 1, 2, 3, 5$ are given in Table I. For $h_{4,q}$, we ob-

TABLE I. Coefficients for the expansions in Eq. (43) of the perturbative structure functions for $W^*q \to QX$.

j	A_j	B_1^j	B_2^j	B_3^j
1	0	$1-4z+z^2$	$z-z^2$	$\frac{1}{2}$
2	$K_A/2$	$2-2z^2-2/z$	$2/z-1-z$	$\frac{1}{2}$
3	0	$-1-z^2$	$1-z$	$\frac{1}{2}$
5	$\frac{\lambda-1-K_A}{2\lambda}$	$-1-z^2$	$3-2z-z^2$	$z-\frac{1}{2}$

tain simply

$$h_{4,q} = \langle \tfrac{4}{3} \rangle \left[1 - \frac{z^2(1-\lambda)^2}{(1-\lambda z)^2} \right]. \tag{45}$$

B. Neutrino-gluon scattering

The $O(g)$ Born graphs for neutrino-gluon scattering are shown in Fig. 2. Following steps analogous to Eqs. (12)–(15), we obtain the corresponding tensor

$$H_G^{\alpha\beta} = \langle \tfrac{4}{8} \rangle \frac{g^2}{2\pi} ds\, d_2 P \sum_{\text{spin}} H_G^{\alpha\dagger} H_G^{\beta}. \tag{46}$$

The factor $\langle \frac{4}{8} \rangle$ arises from color averaging. The spin sum in Eq. (46) is obtained from that in Eq. (15) by crossing. That is, defining

$$F_I^{\alpha\beta} \equiv \sum_{\text{spins}} H^{\alpha\dagger} H^{\beta}[q(p_1) \to Q(p_2) + G(p_3)], \tag{47}$$

$$F_{II}^{\alpha\beta} \equiv \sum_{\text{spins}} H_G^{\alpha\dagger} H_G^{\beta}[G(p_1) \to Q(p_2) + \bar{q}(p_3)], \tag{48}$$

then

$$F_{II}^{\alpha\beta}(p_1,p_2,p_3) = -F_I^{\alpha\beta}(-p_3,p_2,-p_1). \tag{49}$$

Again, we shall present the calculation in detail only for H_1 (to simplify notation, we drop the subscript G). As in Eq. (18), we write

$$H_1 = \frac{g^2}{4\pi} (\mu^{-2\epsilon}) ds\, d_2 P H_1', \tag{50}$$

with

$$H_1' = \frac{2}{t}\left[\frac{2(s-M^2)(Q^2+M^2)}{(s+Q^2)^2} - 1 - \epsilon\right] + 2\frac{1-\epsilon}{u-M^2}\left[\frac{2(1+\epsilon)(s-M^2)(Q^2+M^2)}{(s+Q^2)^2} + \frac{4M^2}{(s+Q^2)} - \frac{8M^2 s}{(s+Q^2)^2} - 1\right]$$
$$+ \frac{4M^2}{(u-M^2)^2}\left(1 - \frac{s+M^2-2\epsilon M^2}{s+Q^2}\right) + \frac{8sQ^2(1-\epsilon)}{(s+Q^2)^3} - \frac{4}{(s+Q^2)} + O(\epsilon^2). \tag{51}$$

We expand the phase-space element as in Eq. (21), use the scaling variables defined in Eqs. (24) and (25), and replace

$$ds = \frac{dz}{z}(s+Q^2) \tag{52}$$

in Eq. (50). The invariant t is expanded as in Eq. (23), and

$$u - M^2 = -\frac{1}{s}(s+Q^2)[M^2 + y(s-M^2)]. \tag{53}$$

The $1/t$ term in Eq. (51) again leads to a β-function singularity for $\epsilon \to 0$. However, the heavy-quark mass M^2 regulates the $u-M^2$ poles in Eq. (51), giving finite terms for $\epsilon \to 0$. Performing the phase-space integrations, we obtain

$$H_1 = 2\langle \tfrac{1}{2} \rangle \frac{\alpha_s}{2\pi}\left(\frac{Q^2+M^2}{4\pi\mu^2}\right)^{\epsilon} \frac{dz}{z}(1-z)^{2\epsilon}(1-\lambda z)^{-\epsilon} z^{-\epsilon} H_1''. \tag{54}$$

The factor $2\langle \frac{1}{2} \rangle$ reflects the conventional normalization of $P_{q/G}$ (below) in which $G \to q$, $G \to \bar{q}$ are counted as individual transitions. The term H_1'' is

$$H_1'' = \frac{1}{2\epsilon}[z^2 + (1-z)^2 + \epsilon]$$
$$+ \tfrac{1}{2}\ln\left(\frac{1-\lambda z}{z-\lambda z}\right)[z^2 + (1-z)^2 + 4z(1-\lambda) - 8\lambda z^2(1-\lambda)]$$
$$+ z(1-z)[3 - 4(1-\lambda)] + \frac{z-\lambda z}{1-\lambda z} - 1 + O(\epsilon). \tag{55}$$

The current-gluon squared matrix element has no

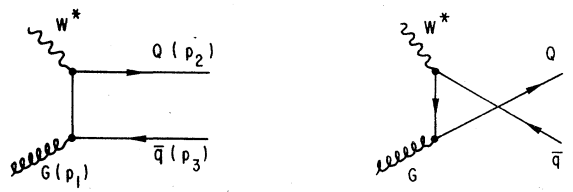

FIG. 2. $O(\alpha_s)$ Born graphs for $W^*G \to Q\bar{q}$.

s-channel poles, so we may simply expand

$$(1-z)^{2\epsilon}(1-\lambda z)^{-\epsilon}z^{-\epsilon} \to 1+2\epsilon\ln(1-z) - \epsilon\ln(1-\lambda z) - \epsilon\ln(z)\,. \tag{56}$$

To put the result for H_1 into a standard form, we introduce the gluon splitting function

$$P_{q/G}(z) = P_{\bar{q}/G}(z) = \langle\tfrac{1}{2}\rangle[z^2+(1-z)^2]\,. \tag{57}$$

We obtain

$$H_1^G = \frac{\alpha_s}{2\pi}\left(\frac{Q^2+M^2}{4\pi\mu^2}\right)^{\epsilon}\frac{\Gamma(1+\epsilon)}{\Gamma(1+2\epsilon)}\frac{dz}{z}\left\{P_{q/G}(z)\left(\frac{1}{\epsilon}+L_\lambda\right)+P_{q/G}(z)[2\ln(1-z)-\ln(1-\lambda z)-\ln z] + 2z(1-2\lambda z)(1-\lambda)L_\lambda + [3-4(1-\lambda)]z(1-z) + \frac{(1-\lambda)z}{1-\lambda z} - \frac{1}{2}\right\}, \tag{58}$$

where

$$L_\lambda \equiv \ln\left[\frac{1-\lambda z}{(1-\lambda)z}\right] \tag{59}$$

and we have reinstated the superscript G.

The perturbative structure functions H_1^G, H_2^G, H_5^G can all be put in a form analogous to Eq. (42):

$$\begin{aligned} H_1^G(z) &= \frac{dz}{z}\left[\mathcal{P}_G(z)+\frac{\alpha_s}{2\pi}h_{1,G}(z,\lambda)\right], \\ H_2^G(z) &= \frac{dz}{z}\left[\mathcal{P}_G(z)+\frac{\alpha_s}{2\pi}h_{2,G}(z,\lambda)\right], \\ H_5^G(z) &= \frac{dz}{z}\left[\mathcal{P}_G(z)+\frac{\alpha_s}{2\pi}h_{5,G}(z,\lambda)\right], \end{aligned} \tag{60}$$

where

$$\mathcal{P}_G(z) \equiv \left(\frac{1}{\epsilon}+L_\lambda\right)\left(\frac{Q^2+M^2}{4\pi\mu^2}\right)^{\epsilon}\frac{\Gamma(1+\epsilon)}{\Gamma(1+2\epsilon)}\frac{\alpha_s}{2\pi}P_{q/G}(z)\,. \tag{61}$$

The residuals h_j are expanded as

$$h_{j,G} = C_0 + C_j^1 z(1-z) + C_j^2 + (1-\lambda)zL_\lambda(C_j^3+\lambda z C_j^4)\,, \tag{62}$$

where

$$C_0 \equiv P_{q/G}(z)[2\ln(1-z)-\ln(1-\lambda z)-\ln(z)]\,. \tag{63}$$

The coefficients C_j^k are given in Table II. For H_3^G, the leading coefficients in the analog of Eq. (51) have opposite signs, giving

$$H_3^G(z) = \frac{dz}{z}\left[\tilde{\mathcal{P}}_G(z)+\left(\frac{\alpha_s}{2\pi}\right)h_{3,G}(z)\right], \tag{64}$$

where

$$\tilde{\mathcal{P}}_G(z) = \left(\frac{1}{\epsilon}-L_\lambda\right)\left(\frac{Q^2+M^2}{4\pi\mu^2}\right)^{\epsilon}\frac{\Gamma(1+\epsilon)}{\Gamma(1+2\epsilon)}\left(\frac{\alpha_s}{2\pi}\right)P_{q/G}(z) \tag{65}$$

and $h_{3,G}$ is expanded as in Eq. (62). Finally, for the finite term H_4^G we obtain

$$H_4^G = \frac{dz}{z}\frac{\alpha_s}{2\pi}h_{4,G}(z)\,, \tag{66}$$

with

$$h_{4,G} = -2z(1-\lambda)L_\lambda + 2(1-z)\,, \tag{67}$$

where L_λ is defined in Eq. (59).

TABLE II. Coefficients for the expansions in Eq. (62) of the perturbative structure functions for $W^*G \to Q\bar{q}$.

j	C_j^1	C_j^2	C_j^3	C_j^4
1	$3-4(1-\lambda)$	$\frac{(1-\lambda)z}{1-\lambda z}-\frac{1}{2}$	2	-4
2	$7-18(1-\lambda)+12(1-\lambda)^2$	$\frac{1-\lambda}{1-\lambda z}-\frac{1}{2}$	6λ	-12λ
3	$-1+2(1-\lambda)$	$\frac{1}{2}$	$-2(1-z)$	2
5	$7-10(1-\lambda)$	$\frac{(1-\lambda)z}{1-\lambda z}-\frac{1}{2}$	4	-10

C. Comments

Equations (41)–(45), Eqs. (58)–(67), and Tables I and II contain the primary results of this section: the perturbative structure functions for heavy-flavor production. These expressions are singular, with the generic form

$$H_j(\text{perturbative}) \sim \frac{1}{\epsilon}P_{a/b}(z) + H_j(\text{finite})\,, \tag{68}$$

where the residual, finite parts are dependent on the scheme used to regularize infrared divergences. The pole term in Eq. (68) has the canonical form required for universal factorization of initial-state collinear singularities. The absorption of these singularities, and the determination of measurable consequences of the finite residuals will be done in Sec. III. There are, however, a few interesting results hidden among the preceeding formulas which merit special comment here.

Identification of the scaling variable

In Eq. (24), we introduced the scaling variable

$$z \equiv \frac{Q^2+M^2}{Q^2+s} = \frac{Q^2+M^2}{2p_1\cdot q}\,. \tag{69}$$

This definition is not arbitrary. Rather, it is required if the initial-state mass singularity $P_{q/q}(z)/\epsilon$ is to be independent of the final state (as required for perturbative factorization). This leads to the flavor-production cross section

$$d\sigma_F(\nu N) \sim \int dx' \tilde{q}(x') d\tilde{\sigma}_F(\nu q) , \tag{70}$$

where $\tilde{q}$ and $d\tilde{\sigma}$ are "regularized" quark distributions, cross sections, and

$$x' = \frac{Q^2 + M_F^2}{2M_N \nu} = x + \frac{M_F^2}{2M_N \nu} . \tag{71}$$

Equations (70) and (71) define a "slow-rescaling" parton-model formalism.[15]

The notion of slow rescaling is by no means new.[16] Our point is simply that it is required for consistency in an on-shell factorized parton model.

Structure-function differences

The regularization-scheme dependence of individual structure functions H_j cancels if we consider differences. Here we examine

$$\Delta(z) \equiv H_2(z)/z - H_1(z) . \tag{72}$$

For quark-current and gluon-current scattering we obtain

$$\Delta_q(z,\lambda) = \frac{\alpha_s}{2\pi} \langle \tfrac{4}{3} \rangle \left[\tfrac{1}{2} K_A \delta(1-z) + 2z + \frac{(1-\lambda)(1+z)(z-2)}{(1-\lambda z)} \right], \tag{73}$$

$$\Delta_G(z,\lambda) = \frac{\alpha_s}{2\pi} \left\{ z(1-z)[4 - 14(1-\lambda) + 12(1-\lambda)^2] + \frac{(1-\lambda)(1-z)}{1-\lambda z} + 2z(1-\lambda)(1-3\lambda) L_\lambda[-1 + 2\lambda z] \right\}, \tag{74}$$

where λ, K_A, L_λ are defined in Eqs. (25), (33), and (59). In the limit $M \to 0$ ($\lambda \to 1$), these agree with the known results:

$$\Delta_q(z) = \frac{\alpha_s}{2\pi} \langle \tfrac{4}{3} \rangle 2z , \tag{75}$$

$$\Delta_G(z) = \frac{\alpha_s}{2\pi} 4z(1-z) . \tag{76}$$

To get some feel for the size of mass effects, we plot $\Delta(z,\lambda)/\Delta(z)$ for several values of λ in Fig. 3.

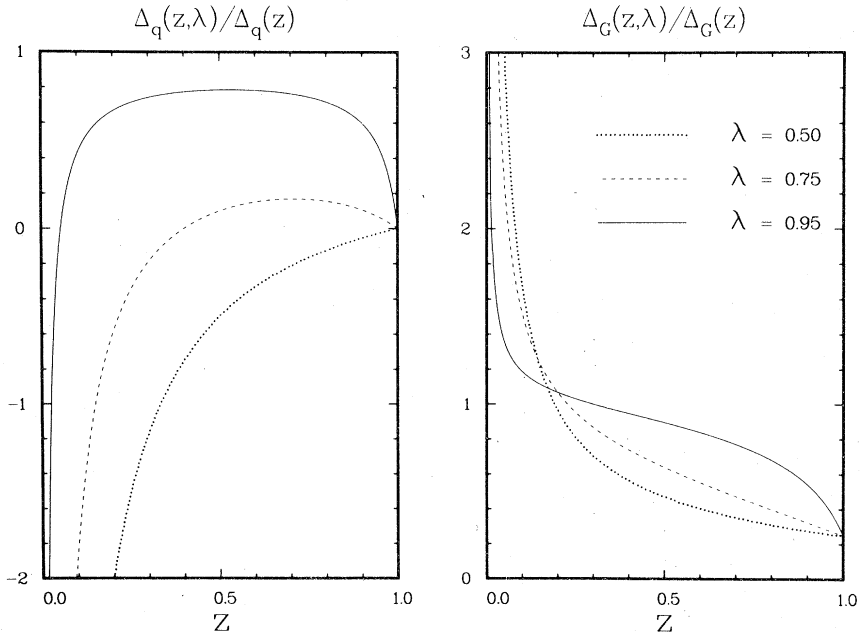

FIG. 3. Ratios of the perturbative structure functions in Eqs. (73) and (74) to the corresponding massless limits for various values of $\lambda = Q^2/(Q^2 + M^2)$.

[The $\delta(1-z)$ component of Δ_q is not used, so that these curves are not reliable for $z \sim 1$.] The $z \to 0$ divergences in Fig. 3 are due to vanishing of Eqs. (75) and (76). Note that the approach to the massless limit is not uniform in z.

Using the longitudinal polarization vector

$$\epsilon_L = (|\vec{q}|, q_0\hat{q})/\sqrt{Q^2} \tag{77}$$

and the form of $H^{\mu\nu}$ in Eq. (10), it is easy to show

$$\epsilon_L^{\mu *}\epsilon_L^{\nu} H^{\mu\nu} = 4(s+Q^2)\left[-H_1 + \left(\frac{s+Q^2}{Q^2}\right)H_2\right] \equiv 4(s+Q^2)H_L , \tag{78}$$

where the longitudinal structure function is

$$H_L(z) = \frac{1}{\lambda z}H_2(z) - H_1(z) . \tag{79}$$

In the massless limit, H_L vanishes to lowest order, and $H_L = \Delta$ is the complete longitudinal structure function through $O(\alpha_s)$. For $\lambda \neq 1$, H_L is not zero for the Born term, so that extraction of $O(\alpha_s)$ corrections must await removal of initial-state singularities from H_j.

While the functions $\Delta(z,\lambda)$ are not simply related to the longitudinal structure function, they are nonetheless of physical interest. The Δ's are kernels (in the sense discussed in Sec. III) for the difference in physical structure functions. Such differences are free from the $O(\alpha_s)$ subtraction-scheme ambiguities which affect individual structure functions.

Connection with massless limit

In the course of deriving the perturbative quark-current and quark-gluon structure functions, we encounter numerous terms of the form

$$\left(\frac{M^2}{Q^2+M^2}\right)^{\epsilon} = (1-\lambda)^{\epsilon} . \tag{80}$$

Such terms do not yield a smooth massless limit:

$$\lim_{\lambda\to 1^-}\lim_{\epsilon\to 0^+}(1-\lambda)^{\epsilon} = 1 , \qquad \lim_{\epsilon\to 0^+}\lim_{\lambda\to 1^-}(1-\lambda)^{\epsilon} = 0 . \tag{81}$$

These noncommuting, ill-defined limits are seen as $\ln(1-\lambda)$ terms in the expansions of real (H_1^R) and virtual (H_1^V) contributions to $H_{1,q}$. While neither H_1^R [Eq. (36)] nor H_1^V [Eq. (37)] has a smooth massless limit, the sum $H_{1,q}$ is completely well behaved for $\lambda \to 1$. This is mandatory, since all singularities associated with $H_{1,q}$ depend on the splitting $q \to qG$ of massless partons.

In contrast, one of the splitting singularities in $H_{1,G}$ is related to heavy-quark production, $G \to Q$. The coefficient of the splitting function is

$$\frac{1}{\epsilon}[1-(s/M^2)^{\epsilon}] \sim L_\lambda + O(\epsilon) . \tag{82}$$

$H_{1,G}$ does not have a smooth massless limit. This "mass ambiguity" is removed only after factorization of the singularity appropriate for $G \to Q\bar{Q}$ splitting.

III. PHYSICAL STRUCTURE FUNCTIONS

The $(1/\epsilon)P_{a/b}(z)$ splitting singularities contained in $H_j^q(z)$ and $H_j^G(z)$ must be absorbed into redefined, effective parton densities. This perturbative factorization will be done in this section. In part A, we briefly review the meaning of parton-model calculations beyond leading-logarithm accuracy in perturbative QCD. In part B, we compute the perturbative electroproduction structure functions needed for implementing the factorization scheme of part A. The results for $\gamma^* q \to qG$ and $\gamma^* G \to q\bar{q}$ are simple and well known. However, for heavy-quark production, $\gamma^* G \to Q\bar{Q}$, factorization is somewhat ambiguous, as we discuss. Finally, in part C we present our final formulas for the QCD-corrected flavor-production structure functions in a compact, usable form.

A. Nonleading corrections to parton-model calculations

In the simple parton model, the cross section for heavy-flavor production in neutrino-nucleon scattering is

$$d\sigma(\nu N \to lFx) = \sum_a \int dx' G_{a/N}(x') d\sigma(\nu a \to lfx) , \tag{83}$$

where f (F) denotes a heavy quark (hadron). The interactions of quarks and gluons described by QCD modify the simple form of Eq. (83). Taking into account only the most singular parts of higher-order amplitudes, the net modification is the now familiar, "factorized" substitution[17]

$$G_{a/N}(x') \to G_{a/N}(x', Q^2) . \tag{84}$$

However, there now exist indications that the simple, factorized picture of leading-logarithm QCD may not be quantitatively adequate for describing physics at presently accessible energies.[2-6] The nonfactorizing pieces of perturbative QCD [e.g., the terms $h_{j,q}(z)$, $h_{j,G}(z)$ of Sec. II] cannot always be neglected. Inclusion of these terms, however, is not completely trivial. Recalling that $h_{j,q}$ is dependent on the specific scheme used to regulate the infrared divergences of perturbative QCD, it is clear that simply adding a term proportional to $h_{j,q}(z)G_{q/N}(z)$ to Eq. (83) can have no physical significance.

The extraction of measurable consequences from

the residuals h_j is discussed in detail in Ref. 2. The algorithm is best described by a simple, schematic example.

Consider two processes involving initial-state nonsinglet quarks. The Born cross sections are

$$d\sigma_j(\text{Born}) = \int dx' d\hat{\sigma}_j^{(0)} q^{(0)}(x') , \tag{85}$$

where $d\hat{\sigma}^{(0)}$ is the lowest-order parton cross section. The perturbative cross sections through next order in α_s can then be written as

$$\begin{aligned} d\sigma_j[O(\alpha_s)] &= \int dx' d\hat{\sigma}_j^{(0)} \int \frac{dz}{z} [\mathcal{P}_q(z) + \alpha_s h_j(z)] q^{(0)}\left(\frac{x'}{z}\right) \\ &= \int dx' d\hat{\sigma}_j^{(0)} \int_{x'}^1 \frac{dy}{y} [\mathcal{P}_q(x'/y) + \alpha_s h_j(x'/y)] q^{(0)}(y) , \end{aligned} \tag{86}$$

where $\mathcal{P}_q$ is a singular function of the general form of Eq. (41), e.g.,

$$\mathcal{P}_q \sim \delta(1-z) + \frac{1}{\epsilon}\left(\frac{\alpha_s}{2\pi}\right) P_{q/q}(z) , \tag{87}$$

if dimensional methods are used to regulate infrared divergences. We now *define* the effective parton distribution by requiring $d\sigma_1[O(\alpha_s)]$ to have the form of Eq. (82):

$$d\sigma_1 \equiv \int dx' d\hat{\sigma}_1^{(0)} q^{(1)}(x') . \tag{88}$$

The parton density beyond leading order is thus

$$q^{(1)}(x') = \int_{x'}^1 \frac{dy}{y} \left[\mathcal{P}_{q/q}\left(\frac{x'}{y}\right) + \alpha_s h_1\left(\frac{x'}{y}\right)\right] q^{(0)}(y) . \tag{89}$$

Since parton distributions are not perturbatively calculable, the relation in Eq. (86) is purely formal. Operationally, the simple product form in Eq. (88) is used to *extract* $q^{(1)}(x')$ from experimental measurements of $d\sigma_1$. The empirical parton densities determined in this manner may be used in calculations of $d\sigma^{(2)}$ provided Eq. (89) is used to eliminate $q^0(y)$ from the $j=2$ version of Eq. (86). Doing this and discarding $O(\alpha_s^2)$ terms gives

$$\begin{aligned} d\sigma_2 = &\int dx' d\hat{\sigma}_2^{(0)} q^{(1)}(x') \\ &+ \alpha_s \int dx' d\hat{\sigma}_2^{(0)} \\ &\times \int_{x'}^1 \frac{dy}{y} \left[h_2\left(\frac{x'}{y}\right) - h_1\left(\frac{x'}{y}\right)\right] q^{(1)}(x') . \end{aligned} \tag{90}$$

The second line in Eq. (90) is independent of regularization schemes used in the calculation, and represents the nonfactorized, measurable correction to leading-logarithm QCD which we seek.

B. Effective parton distributions and perturbative subtractions

Following Ref. 2, we choose to define our effective parton distributions by maintaining the lowest-order expression for the electroproduction structure function F_2:

$$F_2^{\gamma *N}(z)/z \equiv \sum_q e_q^2 G_{q/N}(z) . \tag{91}$$

This has theoretical attractions (e.g., the Adler sum rule is maintained), and the pragmatic advantage that $F_2^{\gamma *N}$ is rather well measured. Difficulties arise in that the quark sea, gluon distributions are not well determined.

To implement this program we need perturbative structure functions for the processes

$$\gamma^* q \to qG , \tag{92}$$

$$\gamma^* G \to q\bar{q} , \tag{93}$$

$$\gamma^* G \to Q\bar{Q} , \tag{94}$$

where, as before, Q (q) denotes a massive (massless) quark. The perturbative H_2 expressions for processes (92) and (93) may be trivially obtained from the $\lambda \to 1$ massless limits of the results in Sec. II.

$\gamma^* q \to qG$:

$$\begin{aligned} \frac{H_2(z)}{z} = \frac{dz}{z} \Bigg[&\delta(1-z) + \frac{1}{\epsilon}\left(\frac{Q^2}{4\pi\mu^2}\right)^{\epsilon} \frac{\Gamma(1+\epsilon)}{\Gamma(1+2\epsilon)} \frac{\alpha_s}{2\pi} P_{q/q}(z) \\ &+ \left(\frac{\alpha_s}{2\pi}\right) h_{2,q}^0(z) \Bigg] , \end{aligned} \tag{95}$$

with

$$\begin{aligned} h_{2,q}^0(z) = \langle \tfrac{4}{3} \rangle \Bigg\{ &-\left(\frac{9}{2} + \frac{\pi^2}{3}\right)\delta(1-z) - \frac{(1+z^2)\ln z}{1-z} \\ &+ (1+z^2)\left[\frac{\ln(1-z)}{1-z}\right]_+ \\ &- \frac{3}{2}\left[\frac{1}{1-z}\right]_+ + 3 + 2z \Bigg\} . \end{aligned} \tag{96}$$

$\gamma^* G \to q\bar{q}$:

$$\begin{aligned} \frac{H_2(z)}{z} = \frac{dz}{z} \Bigg[&\frac{1}{\epsilon}\left(\frac{Q^2}{4\pi\mu^2}\right)^{\epsilon} \frac{\Gamma(1+\epsilon)}{\Gamma(1+2\epsilon)} \frac{\alpha_s}{2\pi} 2P_{q/G}(z) \\ &+ \left(\frac{\alpha_s}{2\pi}\right) h_{2,G}^0(z) \Bigg] , \end{aligned} \tag{97}$$

with

$$h^0_{2,G}(z)=\left[[z^2+(1-z)^2]\ln\left(\frac{1-z}{z}\right)+6z(1-z)\right]. \tag{98}$$

The scaling variable z is given by the massless limit of Eq. (24):

$$z=\frac{Q^2}{Q^2+s}\,. \tag{99}$$

Equations (95)–(98) agree with the corresponding results in Ref. 2.

For $\gamma^*G\to Q\bar{Q}$, the analysis is somewhat ambiguous. The heavy-quark masses regulate infrared divergences, so we may take $\epsilon=0$ from the outset. Following steps analogous to those in the calculations of Sec. II, it is easy to obtain

$$H_2=\frac{\alpha_s}{4\pi}\,ds\left(\frac{P^*_Q}{2E^*_Q}\right)\int_0^1 dy\,\tilde{H}_2\,, \tag{100}$$

where y,s are as defined in Sec. II,

$$E^*_Q=\sqrt{s}/2\,, \tag{101}$$

$$P^*_Q=E^*_Q(1-4M^2/s)^{1/2}\,, \tag{102}$$

and

$$\tilde{H}_2=a_0(\hat{u}^{-1}+\hat{t}^{-1})+a_1M^2(\hat{u}^{-2}+\hat{t}^{-2})+a_2\,, \tag{103}$$

with

$$\hat{t}=(p_G-p_Q)^2-M^2\,,\qquad \hat{u}=(p_G-p_{\bar{Q}})^2-M^2\,, \tag{104}$$

and

$$\begin{aligned}a_0=&-1+(3s+8M^2)/(s+Q^2)\\&-4(s^2-2M^4+5M^2s)/(s+Q^2)^2\\&+2s(s^2-4M^4+6M^2s)/(s+Q^2)^3\,,\end{aligned} \tag{105}$$

$$\begin{aligned}a_1=&2-4(s+M^2)/(s+Q^2)\\&+2s(s+2M^2)/(s+Q^2)^2\,,\end{aligned} \tag{106}$$

$$\begin{aligned}a_2=&-2/(s+Q^2)+14s/(s+Q^2)^2\\&-24s^2/(s+Q^2)^3+12s^3/(s+Q^2)^4\,.\end{aligned} \tag{107}$$

The angular integrations in Eq. (100) are trivial. Problems arise, however, in defining an appropriate scaling variable z. For the massless-quark case, the collinear singularity is an "artificial" $1/\epsilon$ pole. Identifying the coefficient of this pole with a known splitting function fixes the definition of z. In contrast, the singularity for $G\to Q\bar{Q}$ splitting is "physical": $\ln M^2$. Thus, $M^2\ln M^2$ terms from Eq. (105) may be either absorbed into $P_{q/G}(z)\ln M^2$, or left as perfectly acceptable finite residuals.

The scaling variable definition in Eq. (24) is unacceptable, in that the kinematic limit $z\to 1$ yields a negative argument for the square root in Eq. (102). We choose to generalize Eq. (24) by defining

$$z=\frac{Q^2+s_{\rm th}}{Q^2+s}\,, \tag{108}$$

where $s_{\rm th}$ is the hard-scattering threshold ($s_{\rm th}=4M^2$ for $\gamma^*G\to Q\bar{Q}$, vs $s_{\rm th}=M^2$ for $W^*G\to Q\bar{q}$). We maintain the definition of λ in Eq. (25) [replacing M^2 by $s_{\rm th}$ in Eq. (25) gives $F_2(\gamma^*N)\neq F_2(W^*N)$ for $\lambda\to 1$].

Using Eq. (108) in Eqs. (100)–(107) it is straightforward to obtain the required perturbative H_2.

$\gamma^*G\to Q\bar{Q}$:

$$\frac{H_2(z)}{z}=\frac{dz}{z}\left[2L_\lambda\left(\frac{\alpha_s}{2\pi}\right)P_{q/G}(z)+\left(\frac{\alpha_s}{2\pi}\right)k^0_{2,G}(z)\right], \tag{109}$$

where L_λ is defined in Eq. (59), and

$$\begin{aligned}k^0_{2,G}(z)=&\,2P_{q/G}(z)\ln R(\lambda,z)\\&+(1-\lambda)[L_\lambda+\ln R(\lambda,z)]C_A(\lambda,z)\\&+T(\lambda,z)[-1+8z(1-z)]\\&+(1-\lambda)T(\lambda,z)C_B(\lambda,z)\,,\end{aligned} \tag{110}$$

with

$$T(\lambda,z)\equiv P^*_Q/E^*_Q=\left[\frac{(1-z)(4-3\lambda)}{1-\lambda z+3(1-\lambda)}\right]^{1/2}, \tag{111}$$

$$R(\lambda,z)=[1+T(\lambda,z)]^2\left[\frac{4-3\lambda-\lambda z}{4-4\lambda z}\right], \tag{112}$$

$$\begin{aligned}C_A(\lambda,z)=&-(1-5z+9z^2)h_\lambda\\&+(1-\lambda)zh_\lambda{}^2(23z/2-3)\\&-9(1-\lambda)^2z^2h_\lambda{}^3/2\,,\end{aligned} \tag{113}$$

$$\begin{aligned}C_B(\lambda,z)=&(1-17z+25z^2)h_\lambda\\&+(1-\lambda)zh_\lambda{}^2(9-26z)\\&+9(1-\lambda)^2z^2h_\lambda{}^3\,,\end{aligned} \tag{114}$$

where

$$h_\lambda=\frac{4}{4-3\lambda}\,. \tag{115}$$

C. Physical structure functions

We have finally completed all preliminaries and can now give simple formulas for the flavor production structure functions F_j corrected to $O(\alpha_s)$. The connection between the perturbative distributions H_j used above and the structure functions F_j is straightforward. Generalizing the discussion of Sec. III A to include flavor-singlet contributions, we may write for $\mathfrak{F}_j(x)=F_1(x)$, $F_2(x)/x$, $-F_3(x)$, and $F_5(x)$:

$$\mathcal{F}_j(x)/2 = \hat{q}(x) + \int_x^1 \frac{dz}{z} K_j^q(\lambda, z)\hat{q}(x/z) + \int_x^1 \frac{dz}{z} K_j^G(\lambda, z)\hat{G}(x/z)\,. \tag{116}$$

The terms $\hat{q}, \hat{G}$ are (physical) parton densities weighted by weak-coupling strengths [e.g., $\hat{q}(x) = \sin^2\theta_C d(x) + \cos^2\theta_C s(x)$ for charm production in the four-quark model]. The kernels K_j^q, K_j^G are obtained by subtracting the electroproduction perturbative distributions of Sec. III B from the perturbative distributions of Sec. II:

$$K_j^q = \tilde{H}_j^q(W^*q \to Q(G)) - H_2^q(\gamma^*q \to qG)/z\,, \tag{117}$$

$$K_j^G = \tilde{H}_j^G(W^*G \to Q\bar{q}) - \tfrac{1}{2} H_2^G(\gamma^*G \to q\bar{q})/z - \tfrac{1}{2} H_2^G(\gamma^*G \to Q\bar{Q})/z\,, \quad (j \neq 3) \tag{118}$$

$$K_3^G = \tilde{H}_3^G(W^*G \to Q\bar{q}) - \tfrac{1}{2} H_2^G(\gamma^*G \to q\bar{q})/z + \tfrac{1}{2} H_2^G(\gamma^*G \to Q\bar{Q})/z\,, \tag{119}$$

where $\tilde{H}_j \equiv H_j$ for $j \neq 2$, and $\tilde{H}_2(z) \equiv H_2(z)/z$. Note that in Eqs. (118) and (119), the subtractions are related to underlying transitions $W^*q \to Q$ and $W^*\bar{Q} \to \bar{q}$. This accounts for the relative minus sign in the last two terms of Eq. (119).

In order to expand the kernels K^q, K^G in a numerically useful form we use the identity

$$\int_x^1 dz\, f(z)[h(z)]_+ = \int_x^1 dz[f(z) - f(1)]h(z) - f(1)\int_0^x dz\, h(z)\,. \tag{120}$$

This suggests introducing a modified distribution $[h(z)]_{(x)}$, with

$$\int_x^1 dz\, f(z)[h(z)]_{(x)} \equiv \int_x^1 dz[f(z) - f(1)]h(z)\,. \tag{121}$$

The kernels in Eq. (116) can now be listed rather simply:

$$K_j^q(\lambda, z, x) = \langle \tfrac{4}{3} \rangle \frac{\alpha_s}{2\pi} \hat{K}_j^q(\lambda, z)\,, \tag{122}$$

$$\hat{K}_j^q = \hat{A}_j\delta(1-z) + (1+z^2)\left[\frac{\ln(1-z) - \ln(1-\lambda z)}{(1-z)}\right]_{(x)} + [B_1^j - (1+z^2)\ln\lambda - 3/2 + z + 2z^2]\left[\frac{1}{1-z}\right]_{(x)} + B_2^j/(1-\lambda z) + B_3^j\left[\frac{1-z}{(1-\lambda z)^2}\right]_{(x)}\,, \tag{123}$$

where

$$\hat{A}_j = A_j - \tfrac{3}{2}\ln\lambda - \left(\frac{1-\lambda}{2\lambda}\right) - \left(\frac{1+3\lambda}{2\lambda}\right)K_A(\lambda) - (\tfrac{1}{2} + 4\ln\lambda)\ln(1-x) + \left[\ln(1-\lambda x) + \frac{\lambda(1-\lambda)x}{1-\lambda x}\right]\left(\frac{1}{2\lambda^2}\right) - 2\,\mathrm{Li}_2\left[\frac{\lambda-1}{\lambda(1-x)}\right] + 2\,\mathrm{Li}_2\left(1 - \frac{1}{\lambda}\right). \tag{124}$$

The coefficients A_j, B_n^j are given in Table I. $K_A(\lambda), \lambda$ are defined in Eqs. (33) and (25). Note the x dependence in $K_j^q(\lambda, z, x)$ introduced via Eqs. (120) and (121). For K_j^G we have

$$K_j^G(\lambda, z) = \frac{\alpha_s}{2\pi}\hat{K}_j^G(\lambda, z)\,. \tag{125}$$

For $j \neq 3$,

$$\hat{K}_j^G(\lambda, z) = \tfrac{1}{2}[z^2 + (1-z)^2][\ln(1-z) - \ln(1-\lambda z) - \ln\lambda - \ln R(\lambda, z)] + z(1-z)[C_j^1 - 3 - 4T(\lambda, z)] + C_j^2 + T(\lambda, z)/2 + (1-\lambda)L_\lambda[zC_j^3 + \lambda z^2 C_j^4 - C_A/2] - (1-\lambda)[C_A \ln R(\lambda, z) + C_B T(\lambda, z)]/2\,. \tag{126}$$

For $j = 3$,

$$\hat{K}_3^G(\lambda, z) = \tfrac{1}{2}[z^2 + (1-z)^2][\ln(1-z) - \ln(1-\lambda z) - \ln\lambda + \ln R(\lambda, z)] + z(1-z)[C_3^1 - 3 + 4T(\lambda, z)] + C_3^2 - T(\lambda, z)/2 + (1-\lambda)L_\lambda[zC_3^3 + \lambda z^2 C_3^4 + C_A/2] + (1-\lambda)[C_A \ln R(\lambda, z) + C_B T(\lambda, z)]/2\,. \tag{127}$$

L_λ is defined in Eq. (59). The coefficients C_j^n are given in Table II. $T(\lambda, z)$, $R(\lambda, z)$, C_A, and C_B are defined in Eqs. (111)–(114).

Finally, we consider the structure function F_4. Since $F_4 \equiv 0$ to lowest order, the subtractions represented by Eq. (89) do not contribute to $O(\alpha_s)$, and we obtain simply

$$F_4(x) = \left(\frac{\alpha_s}{2\pi}\right)\int_x^1 \frac{dz}{z} h_{4,q}(z) z\hat{q}(x/z) + \left(\frac{\alpha_s}{2\pi}\right)\int_x^1 \frac{dz}{z} h_{4,G}(z) z\hat{G}(x/z)\,. \tag{128}$$

$h_{4,q}$ and $h_{4,G}$ are given in Eqs. (45) and (67).

D. Alternate subtraction schemes

Details of the kernels K^G, K^q depend on specifics of the perturbative subtractions in Eqs. (117)–(119). We can briefly investigate some of this prescription dependence by considering two different schemes.

No heavy-quark subtractions

In the spirit of the factorized parton model, the subtracted term for $\gamma^*G \to Q\bar{Q}$ [Eq. (109)] is implicitly identified with the Q^2 evolution of the heavy-quark sea. A complete treatment of neutrino flavor production should thus also include

the spectator graphs shown in Fig. 4. These graphs pose phenomenological problems, in that the kinematic properties of the flavored fragments are essentially unknown. To avoid such difficulties, we can consider a perturbation calculation without heavy-quark subtractions. The kernels in Eqs. (126) and (127) are replaced by

$$\tilde{K}_j^G(z,\lambda)=P_{q/G}(z)[\ln(1-z)-\ln(1-\lambda z)-\ln\lambda\pm L_\lambda] + z(1-z)(C_j^1-3)+C_j^2+(1-\lambda)zL_\lambda(C_j^3+\lambda z C_j^4)\,. \tag{129}$$

The $-L_\lambda$ choice is for $j=3$. This scheme assumes the nucleon has no intrinsic charmed sea.

Modified subtraction scales

The subtractions in Sec. III C are done at fixed Q^2, which means different scales Q^2/μ^2, $(Q^2+M^2)/\mu^2$ in the sense of renormalization-group analysis. This is the origin of terms proportional to $-\ln\lambda P_{a/b}(z)$ in K^q, K^G. We can construct modified kernels $K_j \sim H_j^{W*}(Q^2)-H_j^{\gamma*}(Q^2+M^2)$ by simply deleting the $\ln\lambda P_{a/b}(z)$ terms from Eqs. (122)–(127).

Implications of both modified subtraction schemes will be discussed in the following section.

IV. RESULTS FOR CHARM

We now investigate some of the implications of the formulas in Sec. III C for charm production in the four-quark Glashow-Iliopoulus-Maiani model. Higher-order leading-logarithmic QCD effects could be included in the calculation by using Q^2-dependent parton densities and an effective coupling $\alpha_s(Q^2)$ as determined from fits to νW_2 electroproduction data. For our purposes, however, this represents an unnecessary refinement (indeed, uncertainties in the flavor dependence of the sea are larger than effects related to Q^2 evolution), so we use instead a simple scaling form (for an isoscalar nucleon target):

$$\begin{aligned} &u(x)=d(x)=V(x)+S(x)\,,\\ &\bar{u}(x)=\bar{d}(x)=s(x)=\bar{s}(x)=S(x)\,,\\ &c(x)=\bar{c}(x)=0\,. \end{aligned} \tag{130}$$

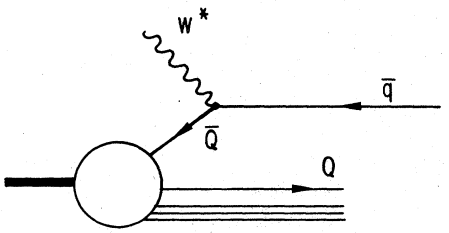

FIG. 4. Spectator, nonparton graph for heavy-flavor production.

We use the valence (V) and sea (S) fits of Ref. 18,

$$xV(x)=\sqrt{x}\,[0.895(1-x)^3(1+2.3x) + 0.535(1-x)^{3.1}]\,, \tag{131}$$

$$xS(x)=0.150(1-x)^7\,. \tag{132}$$

Note that we have taken the charm sea to be identically zero. As we shall see below, the size of the factorized $\gamma^*G\to Q\bar{Q}$ term suggests that this is a reasonable approximation for presently available incident neutrino energies. Finally, for the gluon density we use the counting rule form

$$xG(x)=0.483(N_G+1)(1-x)^{N_G}\,, \tag{133}$$

with $N_G=5$.

A. Structure functions

In Fig. 5 we plot the ratios of corrected to lowest-order structure functions F_2/F_2^0 for several values of $\lambda=Q^2/(Q^2+M^2)$. As is required by our choice of subtraction schemes, Eqs. (117) and (118), the corrections vanish in the limit $\lambda\to 1$, although convergence to this limit is clearly not uniform. The small-x' regions for both $\nu,\bar{\nu}$ are controlled by gluons through K_2^G. The large-x' region for νN is dominated by $\hat{A}_j$ in Eq. (124). For $\lambda<1$,

$$\hat{A}_j \underset{x'\to 1}{\longrightarrow} -(\tfrac{1}{2}+4\ln\lambda)\ln(1-x')-2\,\mathrm{Li}_2\left[\frac{\lambda-1}{\lambda(1-x')}\right] \sim -(\tfrac{1}{2}+4\ln\lambda)\ln(1-x')+\ln^2(1-x')\,. \tag{134}$$

In turn, this behavior can be traced to a term $(P_Q^*/E_Q^*)^\epsilon$ in the phase-space factor, Eq. (21). Summing higher-order $Q\to QG$ radiations may thus be expected to soften this singularity. For $F_2(\bar{\nu}N)/F_2^0$, $\hat{q}(x')=S(x')$, and for large x' the gluon contribution overwhelms the Born term. Since K^G is negative at large z, the "corrected" $F_2(\bar{\nu}N)$ becomes negative at large x', indicating that the uncorrelated sea, gluon densities in Eqs. (132) and (133) are too simplistic to realistically describe the large-x' behavior of sea-dominated processes.

It is convenient here to consider the effects of the different subtraction schemes discussed in Sec. III D. In Fig. 6 we present the F_2/F_2^0 ratios computed with subtraction scale Q^2+M^2. The differences between Figs. 5 and 6 are greatest for small λ, as expected. For $\lambda\gtrsim 0.7$, the two subtraction schemes yield quantitatively similar results. In subsequent calculations, we will use the Q^2 subtraction scale only.

In Fig. 7 we show the F_2/F_2^0 ratios computed without charm-sea factorization. These curves have no $\lambda\to 1$ limit. The heavy-quark kernel $H_2(z,\lambda)$ in Eq. (109) is a positive function which,

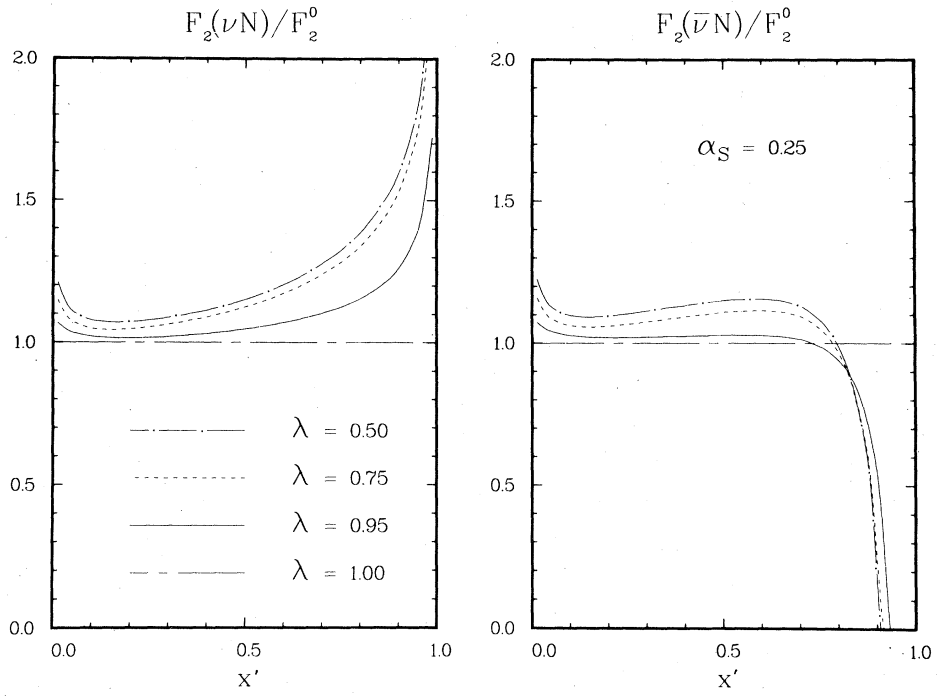

FIG. 5. Ratios of corrected to lowest-order structure functions F_2/F_2^0 for charm production by neutrinos and antineutrinos. The parameter λ is $\lambda = Q^2/(Q^2+M^2)$. The curves are computed using the full kernels as defined in Eqs. (122)–(127).

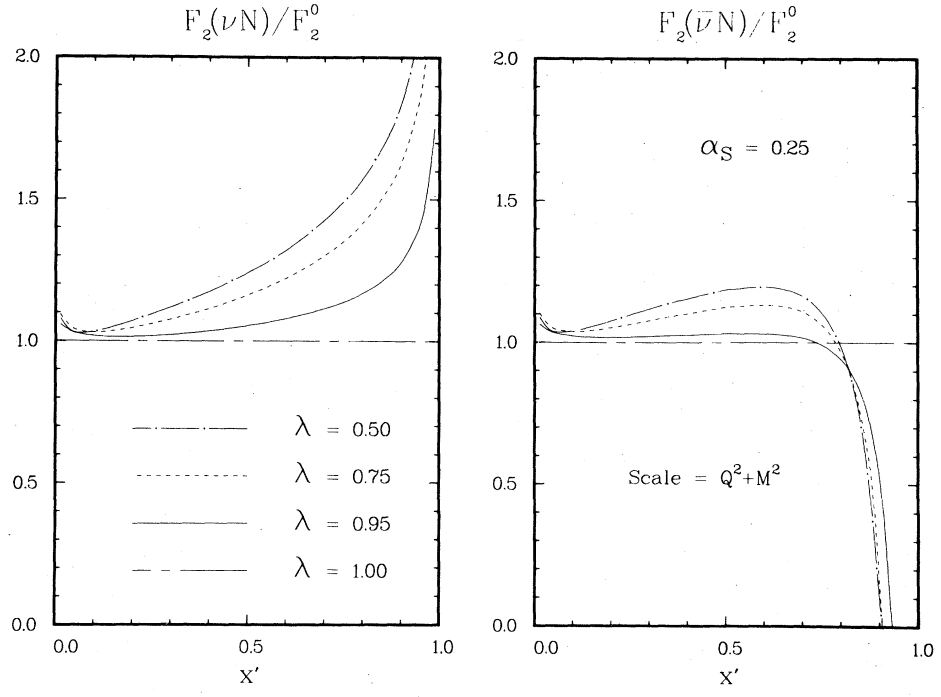

FIG. 6. Corrections to charm-production structure functions F_2 for perturbative subtractions at scale Q^2+M^2 rather than Q^2.

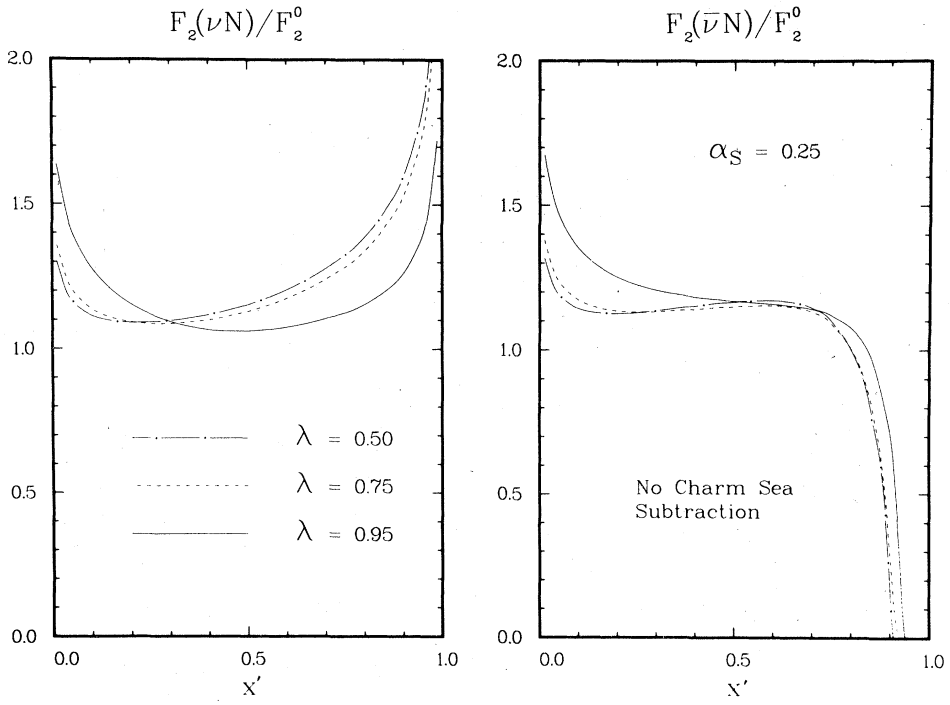

FIG. 7. Corrections to the charm-production structure functions F_2 without subtraction of a charm-sea component.

for fixed z, increases with increasing λ and, for fixed λ, decreases monotonically to zero for $z \to 1$. Accordingly, the curves in Fig. 7 are everywhere higher than the corresponding curves in Fig. 4, with the differences decreasing rapidly for increasing x'.

For $0.6 \lesssim \lambda \lesssim 0.9$ (corresponding to the bulk of presently available charm-dimuon data), the behavior of $F_2/F_2^0(\nu N)$ for $0.4 \lesssim x' \lesssim 0.9$ is largely insensitive to modifications in the subtraction scheme. This is also true for corrections to F_1, F_3.

In Fig. 8 we show results for F_1/F_1^0, using the fully subtracted kernels in Eqs. (122)–(127). In the limit $\lambda \to 1$, the corrections to F_1, F_3 are simple:

$$x'F_1(x') = F_2(x') - \left(\frac{\alpha_s}{2\pi}\right)\left[\tfrac{8}{3}x'^2\int_{x'}^1 \frac{dz}{z^3}F_2(z) + 8x'^2\int_{x'}^1 \frac{dz}{z^2}\left(1-\frac{x'}{z}\right)G(z)\right], \quad (135)$$

$$-x'F_3(x') = F_2(x') - \left(\frac{\alpha_s}{2\pi}\right)\left[\tfrac{4}{3}x'\int_{x'}^1 \frac{dz}{z^2}\left(1+\frac{x'}{z}\right)F_2(z)\right]. \quad (136)$$

For $x' \lesssim 0.4$ and $\lambda \lesssim 0.8$, the curves in Fig. 8 deviate from the massless limit by 20–50%. Also, it is worth noting that gluon contributions which ultimately decouple from F_3 are not negligible for moderate λ. To the extent that m_c^2/Q^2 is not truly negligible, $F_3(\nu N)$ has a nonvanishing singlet component.

B. Charm-production cross sections

We define the charm-excitation ratios

$$R_c(E) \equiv \sigma(\nu \to \mu c)/\sigma(\nu \to \mu) \quad (137)$$

and

$$\Delta R_c \equiv R_c[O(\alpha_s)] - R_c[\text{Born}]. \quad (138)$$

The fractional corrections due to QCD, $\Delta R_c/R_c$, are shown in Fig. 9, where the two sets of curves correspond to different perturbative subtraction schemes: (I) full subtraction, Eqs. (117)–(119) and (II) partial subtraction—no heavy-quark sea, Eq. (129). For scheme (I), the asymptotic values ($E_\nu \to \infty$) of the fractional corrections are

$$\Delta R_c/R_c(\nu) \to -1.45\left(\frac{\alpha_s}{2\pi}\right), \qquad \Delta R_c/R_c(\bar{\nu}) \to -2.07\left(\frac{\alpha_s}{2\pi}\right). \quad (139)$$

For finite E_ν, the behavior of $\Delta R_c/R_c$ is determined both by the λ dependence of the corrected structure functions and by the kinematic limits of heavy-quark production, as discussed in Appendix B. For the parton densities in Eqs. (131)–(133), we obtain

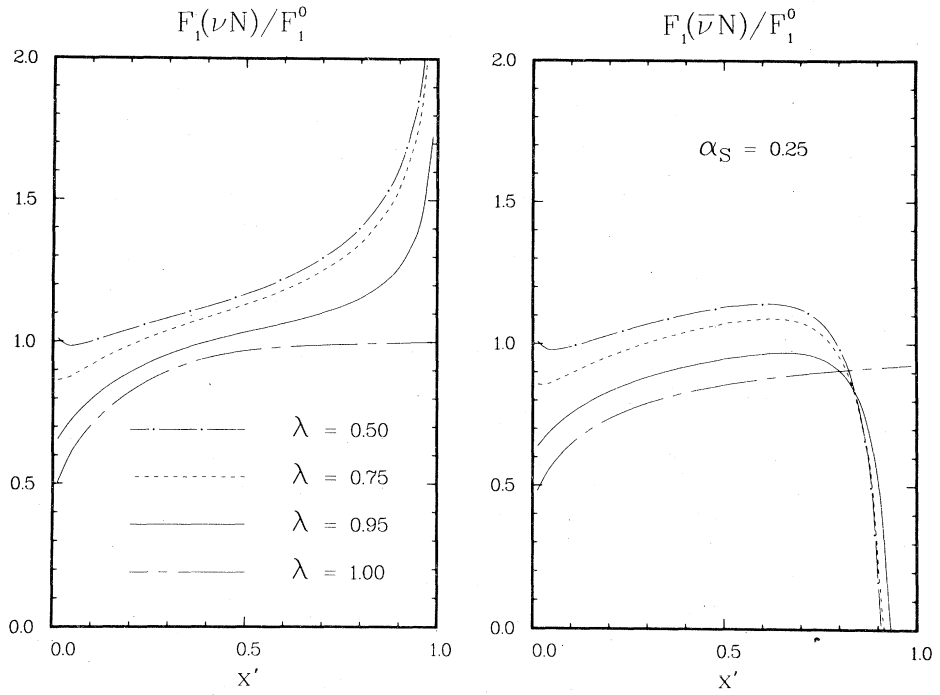

FIG. 8. Corrections to the charm-production structure functions F_1 using the same subtraction scheme as in Fig. 5.

$$\langle\lambda_\nu\rangle = 0.71 \quad (E = 100 \text{ GeV}) \\ = 0.83 \quad (E = 300 \text{ GeV}), \tag{140}$$

$$\langle\lambda_{\bar{\nu}}\rangle = 0.65 \quad (E = 100 \text{ GeV}) \\ = 0.77 \quad (E = 300 \text{ GeV}). \tag{141}$$

For these values, the corrections to the structure functions (Figs. 5–8) are positive except for very small x'. For fixed $\alpha_s = 0.25$, the asymptotic corrections in Eq. (139) are $-5.7\%(\nu)$ and $-8.2\%(\bar{\nu})$. From Fig. 9 it is evident that convergence to the $m_c^2/Q^2 \to 0$ limit is extremely slow.

Comparing the two sets of curves in Fig. 9, we see that uncertainties in the predicted charm-production rates due to different treatments of the heavy-quark sea are very small (3%) at presently accessible energies. The H_2 subtraction term for $\gamma^* G \to Q\bar{Q}$, Eq. (109), is quite small until Q^2 is large enough that L_λ becomes large—at which point factorization *requires* absorption of the L_λ mass "singularity." We conclude from this comparison that estimates of heavy-flavor production based on nonfactored W^* gluon scattering[19] ($W^* G \to c\bar{s}$, $u\bar{b}$, etc) are dominated by mass parameters used for the light quarks and thus are probably not reliable unless *both* quarks are massive.

Finally, we note that the radiative corrections to R_c are not large enough to be phenomenologically significant. For $E > 100$ GeV, the differences between the sets of curves in Fig. 9 are larger than the corrections themselves. [The neglected spectator graph in Fig. 4 will increase R_c slightly for scheme (I). However, a kinematically careful treatment of this process is beyond the scope of this paper.] The corrections to R_c do not pro-

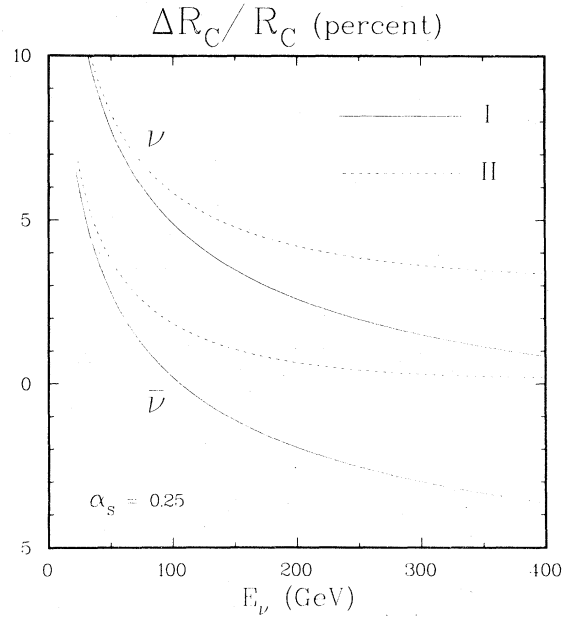

FIG. 9. Fractional changes in the normalized charm-production rate R_c [Eq. (137)] due to QCD radiative corrections. The two sets of curves correspond to different perturbative subtraction schemes, as discussed in the text.

vide a sensitive test of QCD radiative effects.

In Fig. 10 we plot the QCD-corrected charm excitation ratios, using the full-subtraction scheme (I). Over the energy range considered, the R_c values are far below the asymptotic values $0.13(\nu)$ and $0.20(\bar{\nu})$ expected for the input densities in Eqs. (131)–(133). This is a well-known consequence of slow rescaling.[15] Figure 10 also compares the ratio $R_c(\bar{\nu})/R_c(\nu)$ with data[20] for relative dimuon-production rates by neutrinos and antineutrinos. Experimental detection efficiencies in the individual dimuon rates approximately cancel, so that the comparison with "uncut" theoretical predictions is reasonable.

Strictly speaking, Fig. 10 has little to do with QCD radiative corrections: the corresponding curves for the Born terms differ by only a few percent. We have included Fig. 10 to emphasize that, contrary to "popular opinion," *the data in Fig. 10 do not necessarily imply a suppression of the strange sea in the nucleon.* Note that the "fit" in Fig. 10 involves an SU(3)-symmetric sea. Moreover, this curve can be lowered with an SU(3)-symmetric sea fit of the same normalization, $\int dx' x' S(x')$, provided that the $(1-x')^N$ fall off is steeper [e.g., $(1-x')^9$]. Extraction of the size

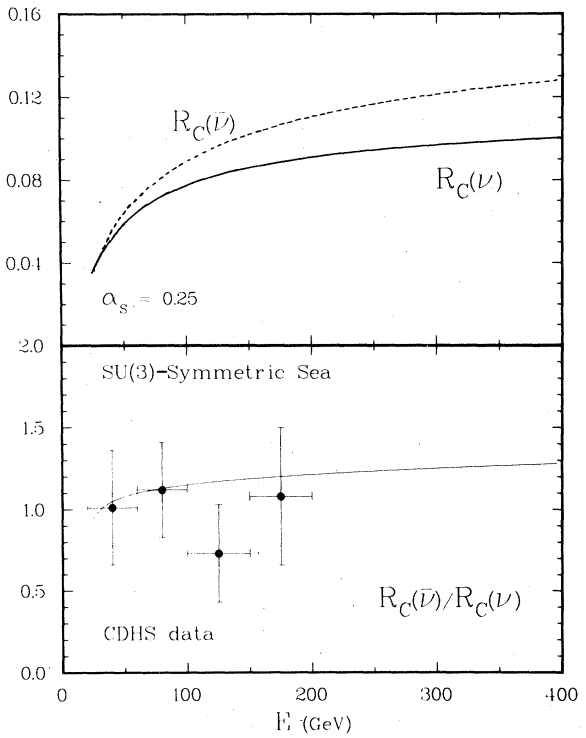

FIG. 10. QCD-corrected charm-production rates, using the input parton densities of Eqs. (130)–(133), and the full perturbative subtraction scheme of Eqs. (117)–(119). The data are from Ref. 20.

of the strange sea must involve fits to $R_c(\bar{\nu})/R_c(\nu)$, $R_c(\bar{\nu})$ itself, and the distribution in the *slow-rescaling* variable x'. Data for such fits should soon be available.[11]

C. Longitudinal structure functions

Dropping terms proportional to the muon mass, the deep-inelastic differential cross section can be put in the form

$$\frac{d^2\sigma}{dx'dy} = \frac{G_F^2 ME}{\pi}[A(x')y^2/2 + B(x')(1-y) + C(x')y(1-y/2)]. \quad (142)$$

Experimental fits to this y dependence are used to extract longitudinal and transverse structure functions:

$$F_T(x') \equiv B(x') = F_2(x'), \quad F_L(x') \equiv B(x') - A(x'). \quad (143)$$

For two generations of massless quarks, the longitudinal structure function is

$$F_L(x') = F_2(x') - x'F_1(x') \quad (144)$$

$$= \left(\frac{\alpha_s}{2\pi}\right)\left[\frac{8}{3}x'^2\int_{x'}^1 \frac{dz}{z^3}F_2(z) + 16x'^2\int_{x'}^1 \frac{dz}{z^2}\left(1-\frac{x'}{z}\right)G(z)\right]. \quad (145)$$

For production of *massive* quarks, Eq. (143) becomes

$$F_L(x',\lambda) = F_2(x') - \lambda x' F_1(x') \quad (146)$$

which agrees (modulo normalization) with Eq. (79). Note that the Born term for Eq. (146) does not vanish for $\lambda < 1$. Thus, although charm production accounts for only about 10% of the total neutrino cross section, the longitudinal structure function for charm seriously obscures the asymptotic QCD expectations of Eq. (145), as demonstrated in Fig. 11. The large-x' "plateaus" in F_L (charm) involve roughly equal contributions from the Born term and radiative corrections. Recalling the caveat after Eq. (134), the behavior for very large x' should not be taken too seriously. Note that the heights of the plateaus essentially scale in $1-\lambda \sim M^2/Q^2$. This behavior could be observable.

V. CONCLUSIONS

The primary objective of this work has been evaluation of lowest-order chromodynamic corrections to heavy-flavor production in deep-inelastic neutrino-nucleon scattering. The principal results of this exercise are the following.

(1) For massless initial-state quanta, universal

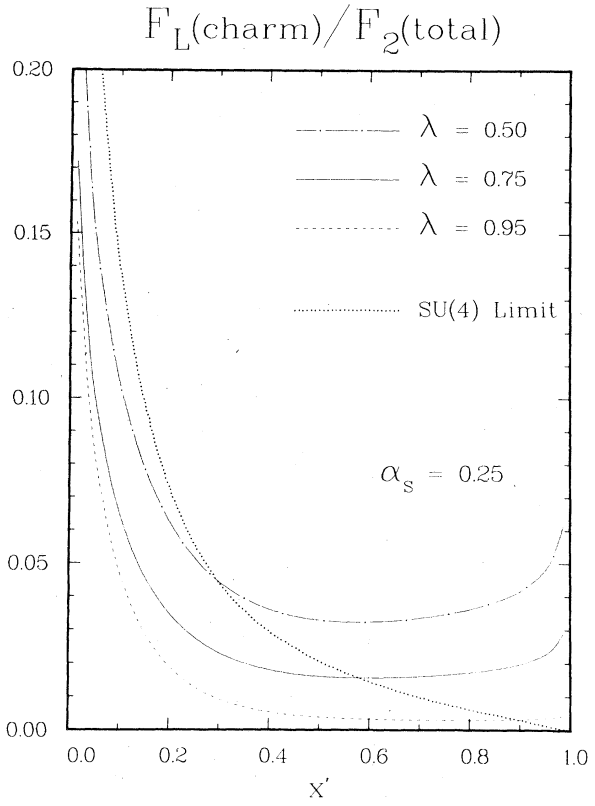

FIG. 11. Longitudinal structure functions for neutrino charm production normalized by the total transverse structure function for inclusive neutrino scattering. The parameter λ is $\lambda \equiv Q^2/(Q^2+M^2)$. For comparison, the *total*, asymptotic F_L for four massless quarks is also shown.

factorization of collinear singularities requires use of the slow-rescaling variable

$$z \equiv \frac{Q^2+M^2}{2p\cdot q} . \tag{147}$$

Residual mass dependence can be conveniently described using

$$\lambda \equiv \frac{Q^2}{Q^2+M^2} . \tag{148}$$

(2) Using the electroproduction structure function F_2 to define the perturbative subtraction scheme, the $O(\alpha_s)$ changes in the flavor-production cross sections are small. Moreover, these corrected total cross sections are rather sensitive to specifics of the perturbative subtraction scheme and thus do not provide good tests of QCD effects.

(3) The subtraction-scheme dependence of the corrected structure functions is largest for $x' \lesssim 0.3$. The 10–30% increases in the neutrino charm-production cross sections for $0.3 \lesssim x' \lesssim 0.8$, $0.6 \lesssim \lambda \lesssim 0.9$ are generally insensitive to the changes in subtraction schemes considered above. This behavior might be observable. The $O(\alpha_s)$ corrections become unreliable for $x' \to 1$. The corrections to sea-dominated processes for $x' \gtrsim 0.5$ are quite sensitive to corrections via initial gluons.

(4) Uncertainties in subtractions related to heavy-quark sea components in the nucleon have little phenomenological effect at presently available incident neutrino energies. The scaling variable appropriate for treatment of the heavy-quark sea is not uniquely specified by perturbative kinematics.

(5) Mass effects make the longitudinal structure function for charm production as large or larger than asymptotic expectations for the total longitudinal structure function for $x \gtrsim 0.2$, $E_\nu \lesssim 300$ GeV.

Although it is not a consequence of QCD corrections, the following seems worth repeating.

(6) Relative rates for dimuon production by neutrinos and antineutrinos are *not* sufficient for extracting the size of the strange-quark sea.

The QCD radiative corrections discussed in this paper have obvious implications for final-state observables in charm-dimuon events. In particular, wide-angle gluon brehsstrahlung should give rise to a power-law tail in $p_T(\mu^+)$, the momentum of the charm-decay muon out of the ν-μ^- production plane. Sufficient dimuon data now exist to see such an effect[11]; quantitative investigations are underway.

ACKNOWLEDGMENTS

It is a pleasure to thank W. Celmaster, S. Gottlieb, D. Jones, and D. Sivers for several useful conversations during the course of this work. Some of the algebraic manipulations and traces were done using ASHMEDAI. This work was performed under the auspices of the United States Department of Energy.

APPENDIX A: VIRTUAL GRAPHS

The amplitude for the vertex correction in Fig. 1(c) is written as

$$\mathfrak{M}^\mu = \bar{u}(p_2)\Lambda^\mu_U(1-\gamma_5)u(p_1) . \tag{A1}$$

We work in the Feynman gauge and use dimensional regularization[12] for both ultraviolet and infrared divergences. It is then straightforward to obtain

$$\Lambda^\mu_U = \left\langle \frac{4}{3} \right\rangle \frac{\alpha_s}{4\pi} \Gamma(1-\epsilon)\left(\frac{Q^2+M^2}{4\pi\mu^2}\right)^\epsilon \times (C_0\gamma^\mu + C_1 p_1^\mu/M + C_q q^\mu/M) , \tag{A2}$$

where

$$C_0=\frac{(1-\lambda)^\epsilon}{\epsilon^2}(1-2\epsilon+4\epsilon^2)-\frac{2}{\epsilon^2}+\frac{3}{\epsilon}$$
$$-8-K_A+2\,\mathrm{Li}_2(\lambda)\,, \tag{A3}$$
$$C_1=2K_A\,, \tag{A4}$$
$$C_q=-2\lambda^{-1}(1-\lambda+K_A)\,. \tag{A5}$$

K_A, λ are as defined in Sec. IIA. The renormalized vertex is $\Lambda_R^\mu=Z_1\Lambda_U^\mu$ with $Z_1=[Z_2(p_1)z_2(p_2)]^{1/2}$. The fermion wave-function renormalization constants are defined on mass shell:

$$Z_2^{-1}\equiv 1-\left.\frac{d\Sigma}{d\not{p}}\right|_{\not{p}=M} \tag{A6}$$

which gives

$$Z_2(M_j)=1+\frac{\alpha_s}{2\pi}\left\langle\frac{4}{3}\right\rangle\left(\frac{M_j^2}{4\pi\mu^2}\right)^\epsilon\frac{\Gamma(1-\epsilon)}{\epsilon}[3-4\epsilon+O(\epsilon^2)]\,, \tag{A7}$$

since $p_1^2=M_1^2=0$, $Z_2(p_1)=1$. For p_2 we write $M^2=(1-\lambda)(Q^2+M^2)$, and thus obtain

$$\Lambda_R^\mu=\frac{\alpha_s}{3\pi}\frac{\Gamma(1+\epsilon)}{\Gamma(1+2\epsilon)}\left(\frac{Q^2+M^2}{4\pi\mu^2}\right)^\epsilon$$
$$\times(C_R\gamma^\mu+C_1p_1^\mu/M+C_qq^\mu/M)\,, \tag{A8}$$

where C_1, C_q are as given above and

$$C_R=\frac{(1-\lambda)^\epsilon}{\epsilon^2}(1-\epsilon/2+2\epsilon^2)-\frac{2}{\epsilon^2}+\frac{3}{\epsilon}-8$$
$$-K_A+2\,\mathrm{Li}_2(\lambda)-\frac{\pi^2}{3}\,. \tag{A9}$$

While we have worked in the Feynman gauge, it is interesting to note that the expressions in Eqs. (A2) and (A7) are in fact unaltered by replacing $-g^{\mu\nu}\to -g^{\mu\nu}+\alpha k^\mu k^\nu/k^2$ for the gluon propagator. With all external lines on shell, the $k^\mu k^\nu/k^2$ piece gives a net contribution of zero to both Λ_U^μ and $Z_2(M^2)$, because of an exact cancellation of ultraviolet and infrared pieces.

The vertex contributions to the parton-level structure functions of Sec. IIA are

$$H_v^j=\left\langle\frac{4}{3}\right\rangle\frac{\alpha_s}{2\pi}\frac{\Gamma(1+\epsilon)}{\Gamma(1+2\epsilon)}\left(\frac{Q^2+M^2}{4\pi\mu^2}\right)^\epsilon\frac{dz}{z}\,\delta(1-z)\tilde{H}_v^j\,, \tag{A10}$$

with

$$\tilde{H}_v^1=C_R\,, \tag{A11}$$
$$\tilde{H}_v^2=C_R+\tfrac{1}{4}C_1\,, \tag{A12}$$
$$\tilde{H}_v^3=C_R\,, \tag{A13}$$
$$\tilde{H}_v^4=0\,, \tag{A14}$$
$$\tilde{H}_v^5=C_R+\tfrac{1}{4}C_q\,. \tag{A15}$$

APPENDIX B: KINEMATIC DETAILS

1. Cross-section formulas

For heavy-flavor production by neutrinos, $\nu N\to lHX$,

$$\frac{d^2\sigma}{dx'dy}=\frac{G_F^2ME}{2\pi}\left\{x'y\hat{y}F_1+2(1-y)F_2\right.$$
$$\left.-\left[x'\hat{y}(2-y)-\frac{M_l^2}{ME}\right]F_3+\frac{M_l^2}{ME}(\hat{y}F_4-F_5)\right\}. \tag{B1}$$

E is the incident neutrino energy, M is the nucleon mass, and

$$y=1-E_l/E\,, \tag{B2}$$
$$\hat{y}=y+\frac{M_l^2-M_H^2}{2x'ME}\,, \tag{B3}$$
$$x'=\frac{Q^2+M_H^2}{2MEy}\,, \tag{B4}$$

where M_l, M_H are the final-lepton, heavy-quark masses. For $\bar{\nu}N$ scattering, the coefficient of F_3 in Eq. (B1) changes sign. For fixed E, the x', y physical region is

$$\frac{(M_l+M_H)^2}{2ME}<x'<1\,, \tag{B5}$$
$$y^\pm=1-\left(1+\frac{x'M}{E}\right)(s'+M_l^2-M_H^2)/(2s')$$
$$\pm\lambda^{1/2}(s',M_l^2,M_H^2)/(2s')\,, \tag{B6}$$

where

$$s'=x'M(x'M+2E) \tag{B7}$$

and

$$\lambda(a,b,c)=a^2+b^2+c^2-2ab-2ac-2bc\,. \tag{B8}$$

2. Projection operators

Working in space-time dimension $D=4+2\epsilon$, we define

$$P_1^{\alpha\beta}=-(s+Q^2)^2g^{\alpha\beta}+4Q^2p_1^\alpha p_1^\beta$$
$$+2(s+Q^2)(p_1^\alpha q^\beta+q^\alpha p_1^\beta)\,, \tag{B9}$$
$$P_2^{\alpha\beta}=-Q^2(s+Q^2)^2g^{\alpha\beta}+4(3+2\epsilon)Q^4p_1^\alpha p_1^\beta$$
$$+2(3+2\epsilon)Q^2(s+Q^2)(p_1^\alpha q^\beta+q^\alpha p_1^\beta)$$
$$+2(1+\epsilon)(s+Q^2)^2q^\alpha q^\beta\,, \tag{B10}$$
$$P_3^{\alpha\beta}=i\epsilon_{\alpha\beta\lambda\kappa}p^\lambda q^\kappa\,, \tag{B11}$$
$$P_4^{\alpha\beta}=p_1^\alpha p_1^\beta\,, \tag{B12}$$
$$P_5^{\alpha\beta}=-(s+Q^2)^2g^{\alpha\beta}+4(3+2\epsilon)Q^2p_1^\alpha p_1^\beta$$
$$+2(2+\epsilon)(s+Q^2)(p_1^\alpha q^\beta+q^\alpha p_1^\beta)\,. \tag{B13}$$

Then, for $H^{\alpha\beta}$ as defined in Eq. (10),

$$P_1^{\alpha\beta}H^{\alpha\beta} = 8(1+\epsilon)(s+Q^2)^3H_1\,, \tag{B14}$$

$$P_2^{\alpha\beta}H^{\alpha\beta} = 8(1+\epsilon)(s+Q^2)^4H_2\,, \tag{B15}$$

$$P_3^{\alpha\beta}H^{\alpha\beta} = -4(s+Q^2)^2H_3\,, \tag{B16}$$

$$P_4^{\alpha\beta}H^{\alpha\beta} = 2(s+Q^2)^2H_4\,, \tag{B17}$$

$$P_5^{\alpha\beta}H^{\alpha\beta} = 8(1+\epsilon)(s+Q^2)^3H_5\,. \tag{B18}$$

The expression in Eq. (B11) is not well defined because of ambiguities in extending $\epsilon_{\alpha\beta\mu\nu}$ to dimensions other than 4.[21] However, the calculations done in this work are sufficiently simple that these ambiguities cause no practical difficulties. In the massless limit, our expression for $xF_3 - F_2$ does reduce to the proper result.[2]

---

[1]For a recent review, see J. Ellis, in *Proceedings of the 1970 International Symposium on Lepton and Photon Interactions at High Energies, Fermilab,* edited by T. B. W. Kirk and H. D. I. Abarbanel (Fermilab, Batavia, Illinois, 1979).

[2]G. Altarelli, R. K. Ellis, and G. Martinelli, Nucl. Phys. B143, 521 (1978); B146(E), 544 (1978); B147, 461 (1979).

[3]J. Kubar-Andre and F. E. Paige, Phys. Rev. D 19, 221 (1979).

[4]R. Barbieri, E. D'Emilio, G. Curci, and E. Remiddi, Nucl. Phys. B154, 535 (1979).

[5]T. Gottschalk, E. Monsay, and D. Sivers, Phys. Rev. D 21, 1799 (1980).

[6]R. K. Ellis, M. A. Furman, H. E. Haber, and I. Hinchliffe, Nucl. Phys. B173, 397 (1980).

[7]W. Celmaster and R. J. Gonsalves, Phys. Rev. Lett. 42, 1435 (1979); Phys. Rev. D 20, 1420 (1979).

[8]W. Celmaster and D. Sivers, Argonne Reports Nos., ANL-HEP-PR-80-28 and ANL-HEP-PR-80-29 (unpublished).

[9]W. A. Bardeen, A. J. Buras, D. W. Duke, and T. Muta, Phys. Rev. D 18, 3998 (1978); W. A. Bardeen and A. J. Buras, *ibid.* 20, 166 (1979).

[10]For a review see M. J. Murtagh, in *Proceedings of the 1979 International Symposium on Lepton and Photon Interactions at High Energies, Fermilab,* edited by T. B. W. Kirk and H. D. I. Abarbanel (Fermilab, Batavia, Illinois, 1979).

[11]Private communication with J. Steinberger [CERN-Dortmund-Heidelberg-Saclay (CDHS) collaboration] and D. Reeder (Harvard-Pennsylvania-Wisconsin-Fermilab collaboration). At the time of this writing the "world supply" of neutrino dimuons is comparable in statistics to the sample of highest-energy continuum events in e^+e^- annihilation.

[12]G. 't Hooft and M. Veltman, Nucl. Phys. B144, 189 (1972); C. G. Bollini and J. J. Giambiagi, Nuovo Cimento 12B, 20 (1972); W. J. Marciano, Phys. Rev. D 12, 3861 (1975).

[13]The importance of maintaining gauge invariance in the context of Drell-Yan calculations is discussed by G. T. Bodwin, C. Y. Lo, J. D. Stack, and J. D. Sullivan, Phys. Lett. 92B, 337 (1980). Gauge-invariant prescriptions for off-shell external lines are discussed by B. Humpert and W. L. van Neerven, *ibid.* 89B, 69 (1979); CERN Reports Nos. CERN-TH-2785 and CERN-TH-2805 (unpublished).

[14]G. Altarelli and G. Parisi, Nucl. Phys. B126, 298 (1977).

[15]R. Barnett, Phys. Rev. Lett. 36, 1163 (1976). For a recent comparison of slow-rescaling predictions with dilepton data see R. Brock, *ibid.* 44, 1027 (1980).

[16]R. Barbieri, J. Ellis, M. K. Gaillard, and G. G. Ross, Nucl. Phys. B117, 50 (1976); H. Georgi and H. D. Politzer, Phys. Rev. D 14, 1829 (1976).

[17]See, for example, C. H. Llewellyn Smith, in *Facts and Prospects of Gauge Theories,* the XVII Schladming Conference on Nuclear Physics, edited by P. Urban (Springer, Berlin, 1978) and references therein.

[18]R. F. Peierls, T. L. Trueman, and L.-L. Wang, Phys. Rev. D 16, 1397 (1977).

[19]J. P. Leveille and T. Weiler, Nucl. Phys. B147, 147 (1979); J. Babcock and D. Sivers, Phys. Rev. D 18, 2301 (1978).

[20]M. Holder *et al.*, Phys. Lett. 69B, 377 (1977).

[21]S. Gottlieb and J. T. Donohue, Phys. Rev. D 20, 3378 (1979); M. Chanowitz, M. Furman, and I. Hinchliffe, Nucl. Phys. B159, 225 (1979).